Nuclear Inst. and Methods in Physics Research B 481 (2020) 62–81

Contents lists available at ScienceDirect

Nuclear Inst. and Methods in Physics Research B

journal homepage: www.elsevier.com/locate/nimb

In situ study of the blistering effect of copper with a thin lithium layer on the neutron yield in the $^{7}Li(p,n)^{7}Be$ reaction

Timofey Bykov[a,b], Nikolay Goloshevskii[c], Sergey Gromilov[d], Dmitrii Kasatov[a,b], Iaroslav Kolesnikov[a,b], Alexey Koshkarev[a,b], Alexandr Makarov[a,b], Alexey Ruktuev[e], Ivan Shchudlo[a,b], Evgeniia Sokolova[a,b], Sergey Taskaev[a,b,*]

[a] Budker Institute of Nuclear Physics, Novosibirsk, Russia
[b] Novosibirsk State University, Novosibirsk, Russia
[c] Institute of Automation and Electrometry, Novosibirsk, Russia
[d] Nikolaev Institute of Inorganic Chemistry, Novosibirsk, Russia
[e] Novosibirsk State Technical University, Novosibirsk, Russia

ARTICLE INFO

Keywords:
Blistering
Charge particle accelerator
Neutron producing target
Boron neutron capture therapy

ABSTRACT

A vacuum insulated tandem accelerator was used to study the effect of blistering on the neutron yield under 2-MeV proton bombardment of lithium target. The target is a thin lithium layer evaporated onto an efficiently cooled copper substrate. Targets with lithium thickness from 1 to 84 μm were irradiated by protons up to fluence of 6.3 10^{20} cm^{-2} which was significantly greater than the blistering threshold. The state of the targets surface was observed using long-distance microscope, video camera, infrared camera. The neutron dose was measured by dosimeters, the neutron flux density was measured by neutron detector. After irradiation, the targets were analyzed on Raman spectrometer, single crystal diffractometer, electron microscope, scanning profilometer, scanning electron microscope, atomic emission spectrometer. The article describes the experiment, presents the results obtained and notes their significance in the enhancement of a target for the neutron source used in boron neutron capture therapy.

1. Introduction

To develop a promising procedure for treating tumors (boron-neutron capture therapy, BNCT [1,2]), an accelerator-based epithermal neutron source has been prepared and designed in the Budker Institute of Nuclear Physics [3–5]. Neutrons are generated as a result of the $^{7}Li(p,n)^{7}Be$ threshold reaction by directing a 2.3 MeV proton beam with a current up to 9 mA, which is produced in the vacuum insulated tandem accelerator, on the lithium target with a diameter of 10 cm. The target consists of a thin lithium layer evaporated in a vacuum on an efficiently cooled substrate (copper, in this case) [6,7]. The thickness of the neutron-generating lithium layer is selected so that the proton energy at the exit of the layer was slightly less than 1.882 MeV, the $^{7}Li(p,n)^{7}Be$ reaction threshold. Further slow down of protons and their absorption occurs in the construction material that must meet the following requirements. Firstly, this material should have a high heat conductivity coefficient or be sufficiently thin for the lithium temperature not to exceed the melting point of 182 °C to prevent the propagation of the formed radioactive beryllium-7 isotope with lithium vapor. From this standpoint, the best material is copper. Secondly, slow down of protons in this material should not cause a significant rise of undesired X-ray and gamma radiation. As a result of the experiments performed [8], it is revealed that the best materials are molybdenum and tantalum, however, it is possible to use copper, too. Thirdly, this material is supposed to be sufficiently resistant to radiation blistering [9–12], i.e. the surface layer deformation expressed as the formation of numerous bulges in the form of elevation and peeling of a thin layer of the material (blisters) under ion bombardment. The appearance of a developed metal surface (blistering) can make the target inapplicable for exploitation [12–15] or limit the operation time [16–21], or cause problems in clinical treatment [22,23]. Various solutions have been proposed for the problem of blistering, the importance of which was emphasized in all publications. For instance, one of them is the use of a target with a thickness less than the total path length proton as in the C-BENS project with 30 MeV protons [24]. In Birmingham [25], Obninsk [26], and Helsinki, on the contrary, the lithium layer is made thick enough to stop protons. However, in most projects, a thin metal layer that is most resistant to radiation blistering (palladium or tantalum, as a rule) is inserted

* Corresponding author at: Budker Institute of Nuclear Physics, Novosibirsk, Russia.
E-mail address: taskaev@inp.nsk.su (S. Taskaev).

https://doi.org/10.1016/j.nimb.2020.08.010
Received 10 April 2020; Received in revised form 7 August 2020; Accepted 19 August 2020

between the neutron-generating layer and the heat removing copper substrate [17,27,28]. Such a diversity of solutions is likely to be due lack of knowledge about the blistering effect on the neutron yield, including the absence of data on the blistering threshold in metals during ~ 2 MeV proton implantation and the metal at temperature near 150 °C (below the lithium melting point). Data on the blistering threshold at these parameters are relevant not only for the lithium target but also the beryllium one because both neutron generation reactions, ^{7}Li(p,n)^{7}Be and ^{9}Be(p,n)^{9}B, considered for BNCT are characterized by similar values of the neutron generation threshold: 1.882 and 2.057 MeV respectively.

We have recently carried out the *in-situ* observation of blistering during 2 MeV proton irradiation of copper and tantalum, and determined for the first time the blistering threshold in copper [29]. The aim of this work was to find out how copper blistering affects the neutron yield from lithium evaporated on copper, as a result of the ^{7}Li(p,n)^{7}Be reaction.

2. Experimental apparatus

Experiments were performed on the vacuum insulated tandem accelerator [4,5] producing a stationary proton beam with an energy up to 2.3 MeV, a current up to 9 mA, and a cross-section of 1 cm. The scheme of the experimental apparatus is shown in Fig. 1.

Sample *7* is placed at the end of the vacuum chamber of the horizontal part of the proton beam transport line. The sample represents a copper disc with a diameter of 144 mm and a thickness of 8 mm. A thin lithium layer with a crystal density and a diameter of 82 mm was evaporated in a vacuum on a copper disc from the side of the proton beam. Four dual-turn spiral channels with a depth of 3 mm and a width of 6 mm and a 1 mm distance between the channels were made on the back side of the copper disc inside of a diameter of 122 mm for water cooling [7]. A planar aluminum disc with a hole in the center to feed cooling water and two holes on the periphery to drain water is attached to the back side of the copper disc. At a characteristic water consumption of 15–17 l/min there is a turbulent water flow with a rate of 3.5–4 m/s in the cooling channels, which ensures an effective heat removing [6].

Lithium is deposited on the target substrate on a evaporation machine by evaporating in a vacuum similar to that described in [30]. After lithium was deposited, the sample together with a part of vacuum chamber *6* closed by gate valve *5* to maintain the vacuum inside is detached from the evaporation machine, carried to the experimental apparatus, and connected with a horizontal part of the proton beam transport line.

The sample is irradiated with a proton beam with a diameter of 10 mm and a current of 500 μA. The current value is limited by the intention to maintain the lithium layer in the solid state to minimize the propagation of the radioactive beryllium-7 isotope across the apparatus. A Faraday cup equipped with nine thermoresistors to control the beam position is moved in the proton beam transport line before sample irradiation. When the proton beam with a current of 500 μA is obtained and the beam is centered, the Faraday cup is moved away and the proton beam irradiates the sample. The proton beam current is measured and controlled by a non-destructive DC current transformer NPCT-CF4″-1/2–47.7–120-UHV (Bergoz Instrumentation, France) (*3* in Fig. 1). The *in-situ* observation of the sample surface is performed by means of a KX InfiniMax™ long-distance microscope (DistaMaxTM, Infinity Photo-optical Co., USA) with a Basler Ace acA4112-30uc CMOS camera through one of branch pipes *6* with a window with fused quartz glass. Through the same branch pipe the sample is enlightened by a 10 W LFP-10WP-R halogen lamp (Shibuya, Japan). Through the second

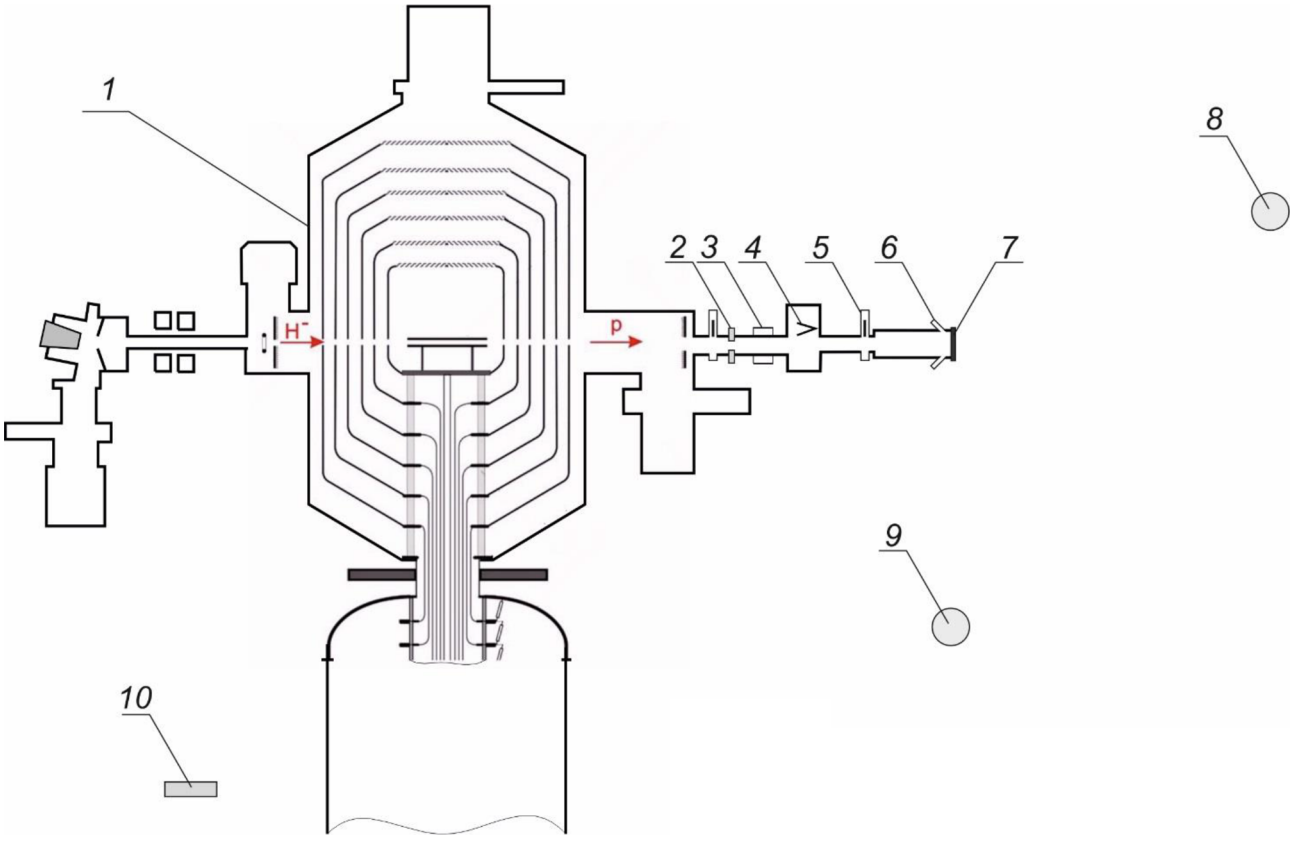

Fig. 1. Scheme of the experimental apparatus: *1* is a vacuum insulated tandem accelerator, *2* is a cooled diaphragm with an aperture of 26 mm, *3* is a contactless current sensor, *4* is a inserted Faraday cup, *5* is a gate valve, *6* are branch pipes with observation windows, *7* is the sample under study, *8* is dosimeter No. 1, *9* is a dosimeter No. 2, *10* is a neutron detector.

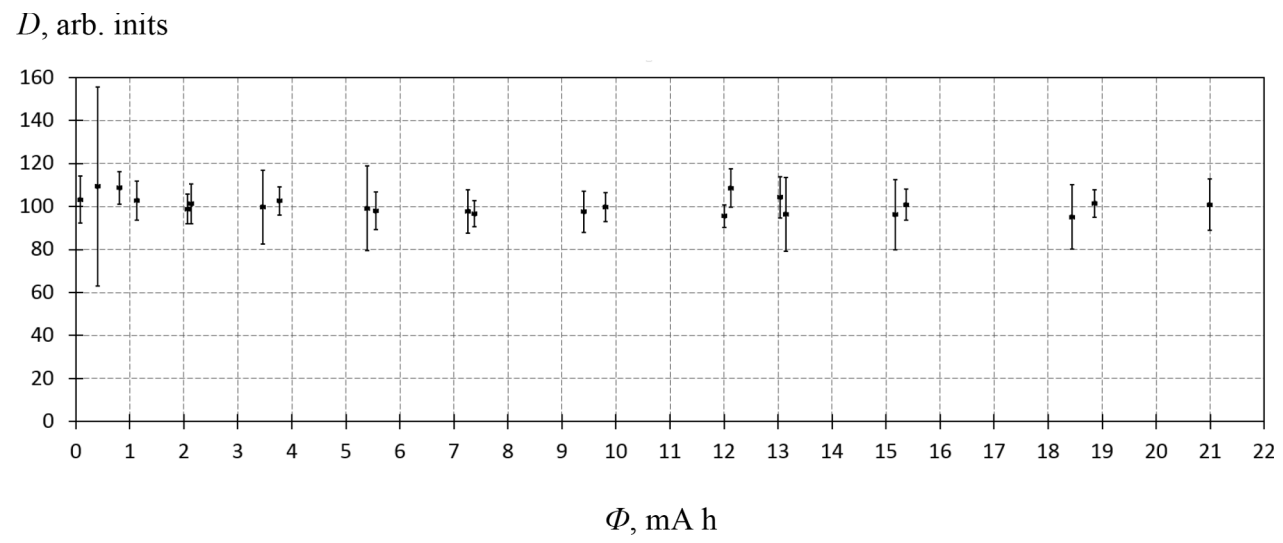

Fig. 2. Dependence of the neutron dose rate D measured by dosimeter No. 1 on the proton current integral Φ.

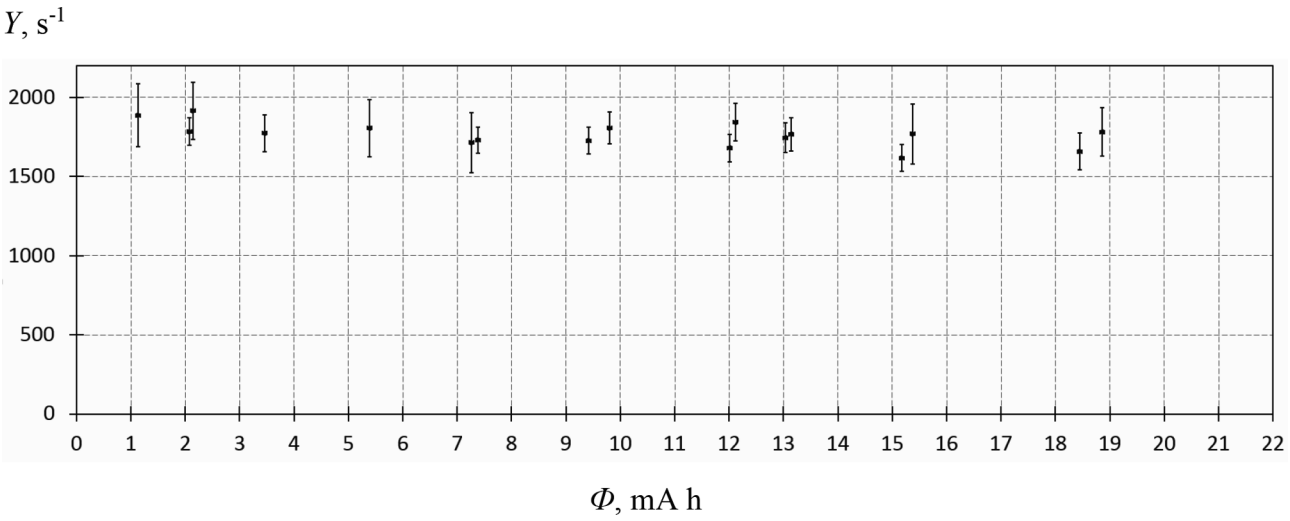

Fig. 3. Dependence of the neutron detector count rate Y on the proton current integral Φ.

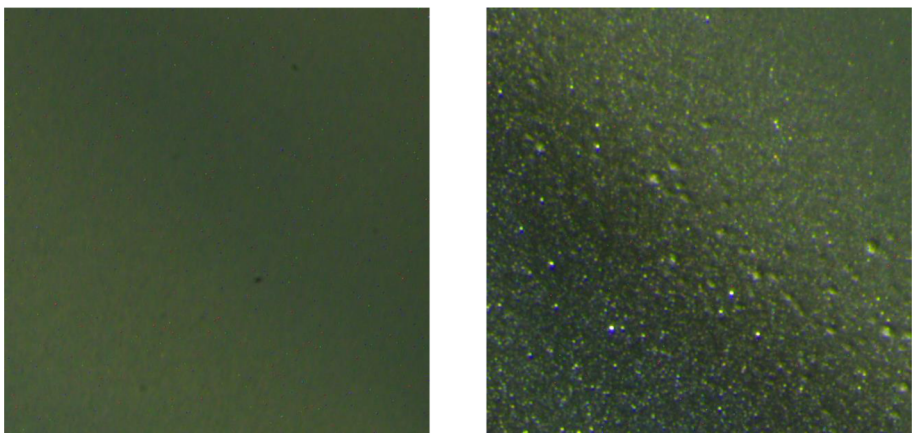

Fig. 4. Target image taken by the long-distance microscope on the 6th day of irradiation: (left) in the center of the proton beam, (right) on the periphery. Image dimensions 50 mm horizontal and 60 mm vertical.

branch pipe with a window with a barium fluoride glass the proton beam position on the sample is first controlled by a FLIR T650sc unfrared camera (FLIR Systems Inc., USA) and then the sample surface is observed by Hikvision DS-2CD4026FWD-AP camera with a Hikvision HV1140D-8MPIR lens.

The ambient neutron dose rate is measured by two BDMN-100–07 detectors (Doza, Russia). Each detector consists of a spherical moderator with a UDMN-100 detection unit placed in it. One of the

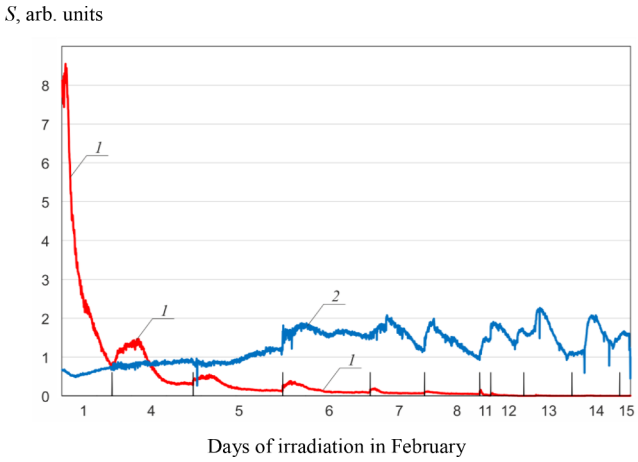

Fig. 5. Dependence of the high brightness area in the chosen part of the image (*1* – in the center of the proton beam, *2* – on the periphery) on the sequence of the processed image frames grouped by irradiation days.

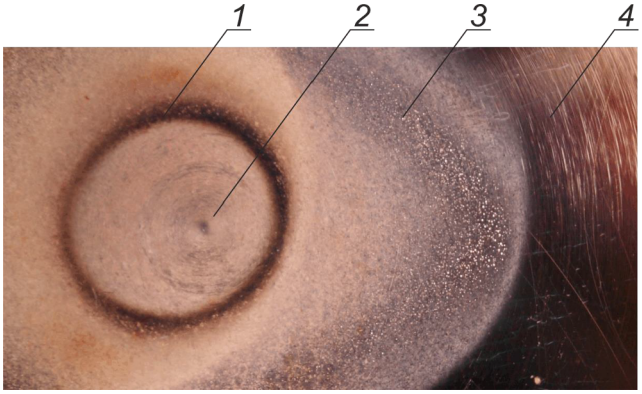

Fig. 6. Image of the sample surface studied: *1* – dark halo, *2* – center of the copper disc, *3* – blisters, *4* – surface not irradiated by protons.

detection units, dosimeter No.1 (*8* in Fig. 1), is placed on a wall of the radiation protected bunker at a distance of 5.4 m from the sample at an angle of 22° to the proton beam direction. The second unit, dosimeter No. 2 (*9* in Fig. 1) is placed at a distance of 1.5 m from the center of the sample at an angle of 90° to the proton beam direction.

The neutron flux is measured by a neutron detector with a GS20 lithium-containing scintillator (The Saint-Gobain Crystals, U.S.A.) mounted on a Hamamatsu R6095 photoelectron multiplier with a high-voltage power supply source MHV12-1.5K1300P (TRACO Electronics, Japan) (*10* in Fig. 1). The detector is located at a distance of 5.46 m from the sample at an angle of 132° to the proton beam direction.

After irradiation, the samples were analyzed on a LabRAM HR Evolution Raman spectrometer (HORIBA Scientific), a Kappa APEX DUO single crystal diffractometer (Bruker, Germany), a DM 5000 electron microscope (Leica, Germany), a scanning profilometer with confocal chromatic sensors developed at the Institute of Automatics and Electrometry (Novosibirsk, Russia), an EVO 50 XVP scanning electron microscope (Zeiss, Germany), and a parallel inductively coupled plasma atomic emission spectrometer with axial and radial plasma viewing ICPE-9820 (Shimadzu, Japan).

2.1. Measurement features

The ^{7}Li(p,n)^{7}Be reaction is a threshold reaction, which means that neutrons are generated at a proton energy exceeding the neutron generation threshold (1.882 MeV in this case). In accordance with the results of calculations given in [31], the neutron yield increases linearly with increasing proton energy from 1.910 to 2.000 MeV: the reliability of the linear approximation of values calculated with a step of 0.01 MeV is $R^2 = 1$. In this proton energy range E_p the neutron yield can be expressed as $Y = 9.5345\ 10^{11}\ (E_p - 1.885)\ \mathrm{mC}^{-1}$ where E_p is substituted in MeV. Note that this straight line of the linear approximation of the data intersects the X-axis at a value of 1.885 MeV that is slightly larger than the reaction threshold of 1.882 MeV.

The linear dependence of the neutron yield on the proton energy is used to calibrate an resistor voltage divider intended to measure the potential fed to the high-voltage electrode of the vacuum insulated tandem accelerator. The potential is measured with a frequency of 1 Hz and applied in the program managing the apparatus to maintain the accelerator high-voltage electrode potential at the set level. In the exploitation of the accelerator it was previously noted that the high-voltage potential, and consequently, the proton energy smoothly decrease during the working day. This seems to be due to a disproportional change in resistances of voltage divider components when it is heated. As it was found in these studies, during 5 h continuous operation of the accelerator at a current of 500 μA the proton energy decreases by 0.65%. This relatively small decrease in the proton energy due to the threshold character of the ^{7}Li(p,n)^{7}Be reaction causes a decrease in the neutron yield by a much larger value of 11%. In order to determine the neutron yield with a higher accuracy than 11%, we calibrated the resistor voltage divider.

The resistor voltage divider was calibrated as follows. The power supply source voltage is set to be $U_1 = 0.95$ MV in the apparatus management program. The 20 keV energy of negative hydrogen ions injected into the accelerator should ensure the production of a proton beam with an energy of 1.92 MeV. In a few minutes, the neutron dose rate D_1 is measured by dosimeter No. 1. Then the voltage is risen to $U_2 = 1.01$ MV, increasing the proton energy to 2.04 MeV, and repeat the measurements of the dose D_2. In the dependence of the dose on the voltage a straight line is drawn through (U_1, D_1) and (U_2, D_2) points up to the intersection with the X-axis and determine the intersection coordinate U_0. If $U_0 \neq U_{thr} = 0.9325$ MV, then it means that the voltage differs from the set value. This difference in the voltages does not exceed 0.65% and is taken into account in the measured neutron yield by an additional term $U_{thr}/U_0 \approx 1$. The neutron yield proportional to the slope of the straight line corresponding to the dependence of the neutron dose on the voltage with regard to the divider calibration correction is calculated as $(D_2 - D_1) \cdot U_{thr}/U_0$.

3. Measurement and results

3.1. Measurement results and discussion. Series I

In the first series of experiments, a lithium layer with a thickness larger than the thickness at which neutrons are generated as a result of the ^{7}Li(p,n)^{7}Be threshold reaction but less than the proton projected range in lithium was evaporated on the copper sample.

When selecting the lithium thickness, we used the expression for the proton energy loss rate S in lithium depending on its energy E [32]:

$$S = \frac{S_{low} \cdot S_{high}}{S_{low} + S_{high}} \mathrm{eV}/(10^{15}\ \mathrm{atoms/cm^2})$$

where $S_{low} = 1.6\ E^{0.45}$, $S_{high} = \frac{725.6}{E} \ln(1 + \frac{3013}{E} + 0.04578\ E)$, E in keV. By means of this formula we obtain that the proton path projected range in lithium is 169 μm for 2.04 MeV proton and 147 μm for 1.882 MeV (note that proton total path length and the projected range practically do not differ). Consequently, at the initial proton energy of 2.04 MeV neutrons are generated up to a depth of 22 μm from the lithium surface. The lithium thickness at which neutrons are generated will be called the neutron generation thickness.

The sample under study was made of 99.996% fine-grained copper (OFC-1 H3150 C1011, SH Coper Products Co., Ltd., Tsuchiura-shi,

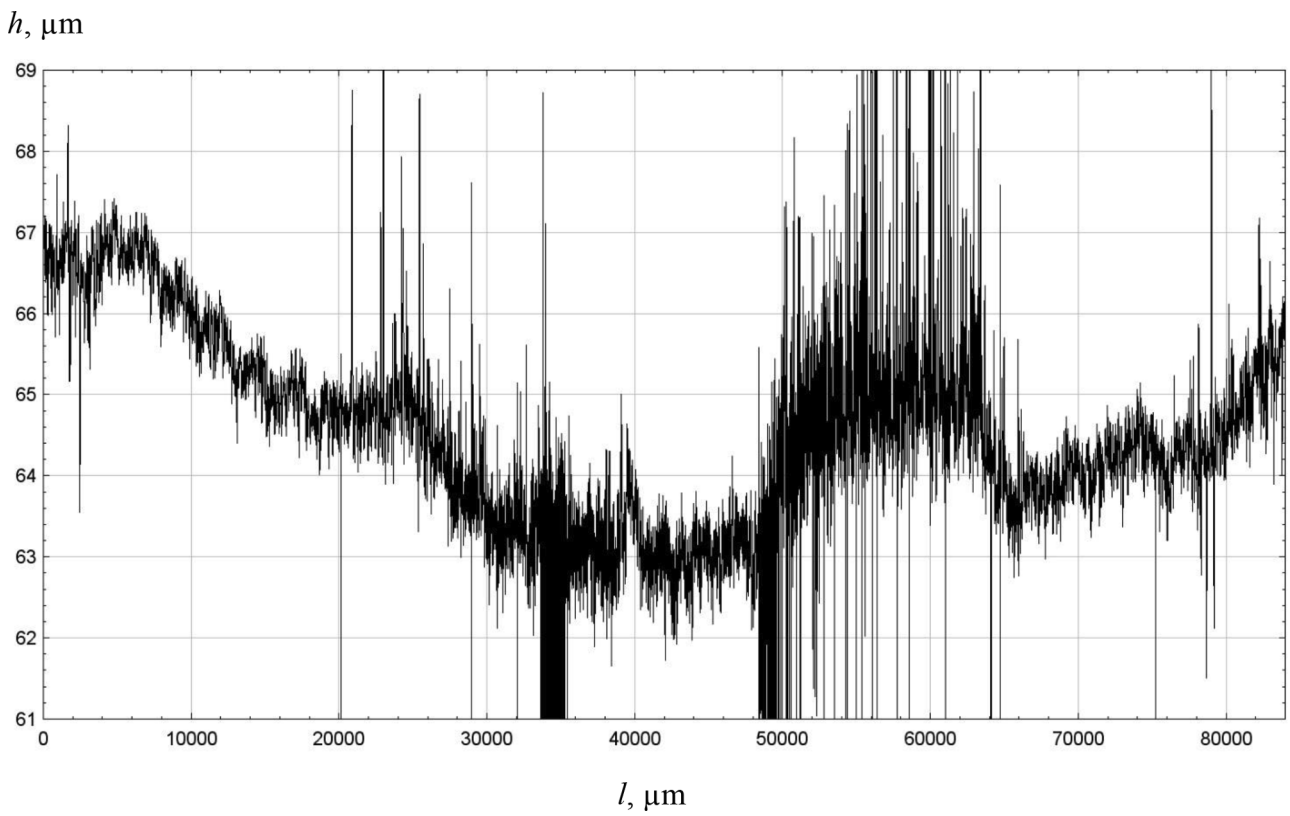

Fig. 7. Sample profile along the line passing through the center of the sample.

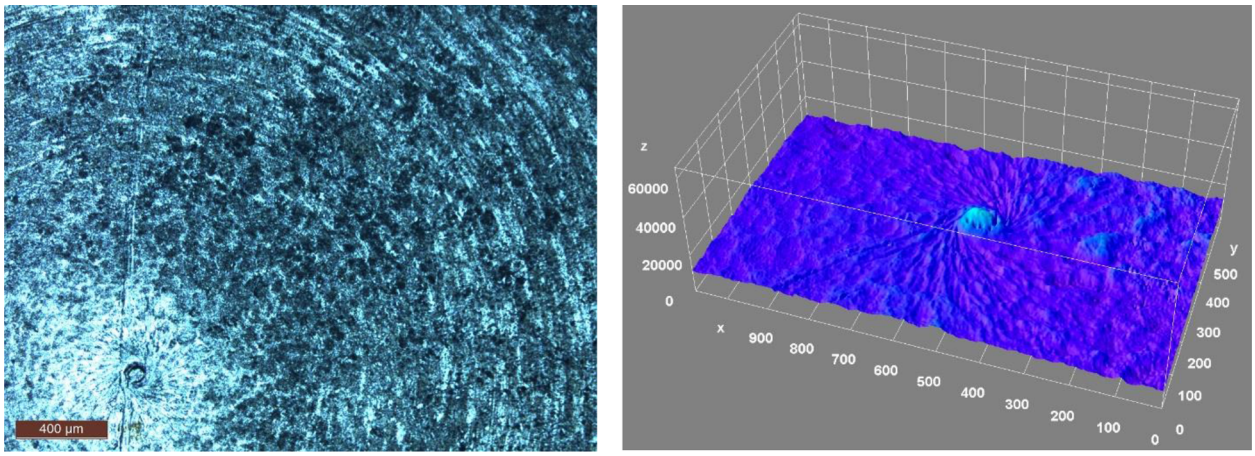

Fig. 8. Image (left) and 2D surface profile of the central part of the target (right).

Japan). A 84 μm thick lithium layer was evaporated on the sample, for which 237 mg of lithium were used. The sample was irradiated by a proton beam with a current of (500 ± 10) μA for 11 days (4 h per day). The integral of current on the sample was 21.08 mA h.

The sample was irradiated by a proton beam at a proton energy of 1.8 MeV, below the neutron generation threshold, and for a short time at larger energies of 1.92 and 2.04 MeV to determine the neutron yield.

Note that in these studies, we obtained a proton beam with parameters similar to those in the *in-situ* observation of copper blistering during implantation of 2 MeV protons [29]. In particular, in [29], from the expansion of boundaries of the region with blisters the effective beam area was determined as the ratio of the current intensity to its maximum density; it amounted to (75 ± 7) mm^2. Taking the beam area to be 75 mm^2, we obtain that at the current integral of 21.08 mA·h the proton fluence was (6.3 ± 0.6) 10^{20} cm^{-2} in the center of the beam.

In [29] it is shown that on the 99.996% copper surface blisters appear starting from the fluence of 0.15 mA h during the implantation of 2 MeV protons. In this case, protons lose a part of energy on lithium and enter into copper with the energy of 1 MeV, stopping in it at a depth of 7 μm [32]. Since the blistering threshold is considered to depend on the energy as $E^{0.4}$ [11], then when copper is implanted with 1 MeV protons, the blisters would appear at a slightly lower fluence of 0.11 mA h.

The dependence of the neutron dose rate measured by dosimeter No. 1 on the proton current integral is shown in Fig. 2. The dependence of neutron detector count rate is shown in Fig. 3.

It was expected [12–23] that after the appearance of blisters the neutron yield could substantially decrease. However, from Figs. 2 and 3 it is seen that there is no expected degradation of the neutron yield.

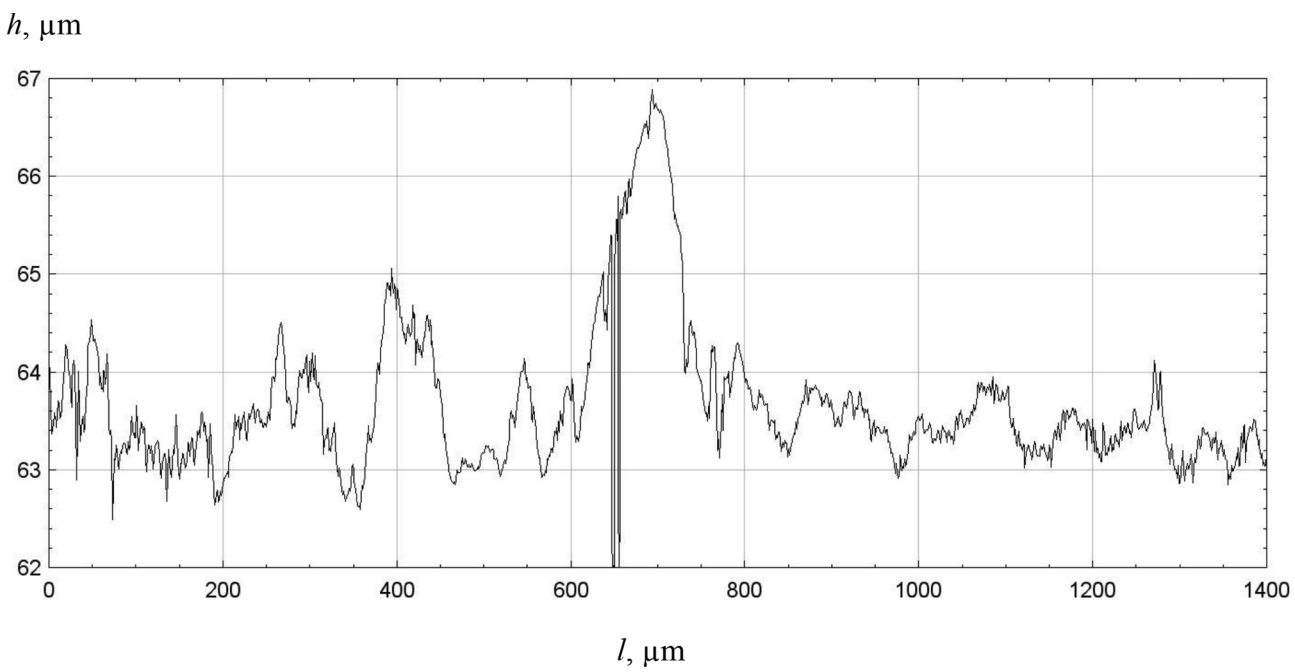

Fig. 9. Surface profile of the central part of the target along the line passing through the center of the target.

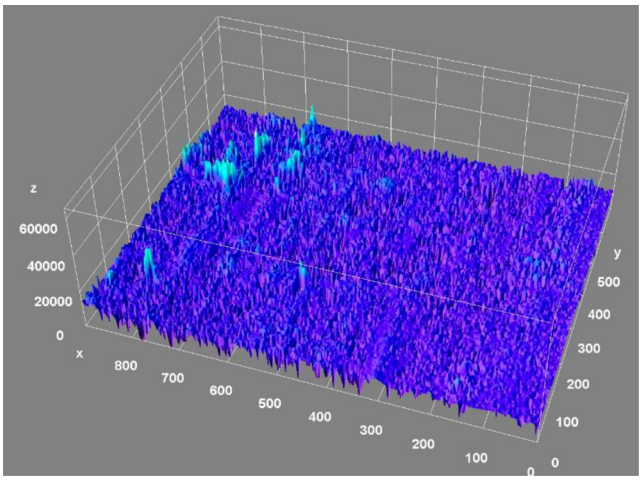

Fig. 10. 2D surface profile of the dark halo.

With an accuracy of 7% it is possible to state that target irradiation to a fluence exceeding the blistering fluence by almost a factor of 200 did not cause degradation of the neutron yield.

Dependences shown in Figs. 2 and 3 allow us to formulate the result that was the primary aim of this study: the appearance of blisters on the surface of the copper substrate of the neutron-generating target with a lithium layer does not result in degradation of the neutron yield.

As for the BNCT problem, this result radically changes the paradigm: blistering does not limit the operation time of the target. In any case, this statement corresponds to the target in the form of a thin lithium layer evaporated on a heat removing copper substrate. The appearance of blisters on the copper surface does not cause degradation of the neutron yield and the target can still be used for therapy of patients (up to 340 patients), as can be predicted from the proton fluence density reached in this experiment at the planned proton current of 10 mA, the target diameter of 10 cm, and the therapy time of 40 min [33]. Note that the use of a target with a lithium layer with a thickness larger than the neutron generation thickness slightly increases a small unwanted dose from 478 keV photons emitted as a result of inelastic scattering of protons by lithium nuclei.

Despite that the main result of the study was achieved, further investigations were carried out to reveal the details of processes yielding this result.

During the entire irradiation time the surface of the sample being studied were monitored by a KX InfiniMax™ long-distance microscope with a Basler Ace acA4112-30uc CMOS camera and a Hikvision video camera, and the video signals were recorded. The appearance and disappearance of blisters were clearly observed in different parts of the target surface. Thus, Fig. 4 shows two regions of the long-distance microscope image on the sixth day of irradiation. It is seen that the lithium surface is homogeneous in the center of the proton beam, with blisters being absent, while blisters are distinct at the periphery of the beam. The lithium surface modification by blisters was quantitatively determined as a high brightness regions in the chosen part of the image. Every 720th frame of the video signal file was processed with a computer, i.e. the images following with a step of 30 s were processed. The processing consisted in distinguishing high brightness regions corresponding to blisters and determining the areas of these regions in two parts of the image: in the center of the beam and on its periphery. The result of processing of the microscope video signal is illustrated in Fig. 5. Here, the ordinate shows the high brightness areas of the chosen part of the image (in the center of the beam and on the periphery) and the abscissa shows the sequence of the processed image frames grouped by days of irradiation: first, February 1, then February 4, and so on until February 15. To make the result visible, vertical lines separating one day of irradiation from another are drawn in the plot. Note that although irradiation was performed for 4 h during 11 days, the number of processed frames in one day is different. This is explained by that on the first day of irradiation the microscope was tuned and because often, especially closer to the end of the experiment, a infrared camera or a pyrometer was mounted on this observation window and the microscope image was not recorded.

It is seen that in the central region of the beam, blisters rapidly appeared on the lithium surface, and then their number began to decrease already on the first day of irradiation. On the next day, their number first increased and then dropped. It was repeated every time, but the amount of blisters was continuously decreasing up to their complete absence on the last two days of irradiation.

Smooth growth of the number of blisters was observed on the

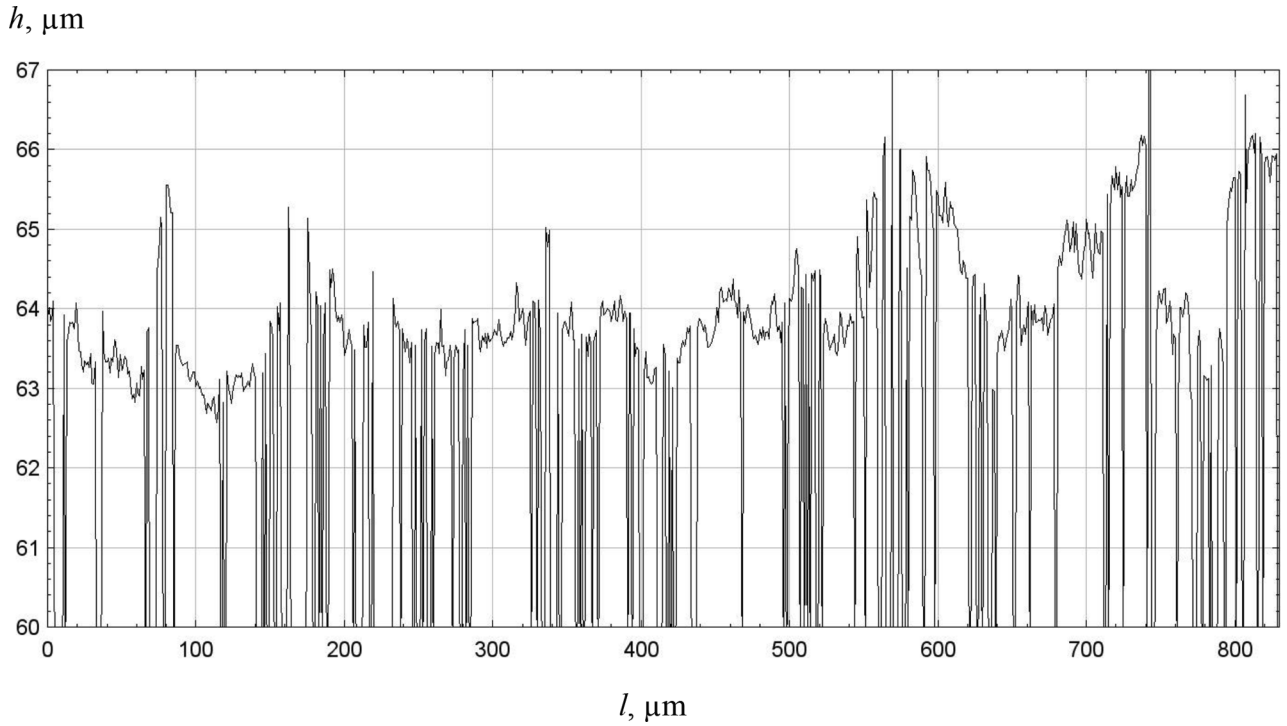

Fig. 11. Surface profile of the dark halo.

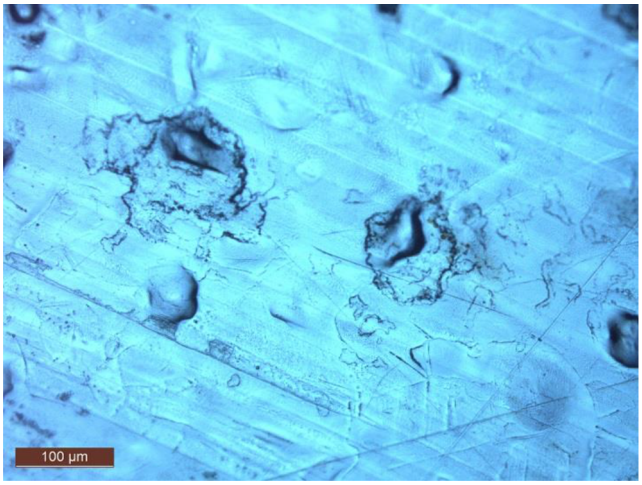

Fig. 12. Image of the copper surface taken on the DM 5000 Leica electron microscope.

periphery during the first three days of irradiation. Then there were similar periodical fluctuations when their number first increased during the day and decreased later, returning to the previous level.

After the completion of irradiation the studied sample was taken out and placed in the atmosphere medium. The most part of the lithium surface was almost immediately blackened – it was not irradiated by the proton beam. The central part of the sample irradiated by the beam looked gray (silvery) with some amount of darker spots, brown in one place.

By means of a steel needle 0.3–0.5 mm particles were taken from different parts of the lithium layer and analyzed on a Kappa APEX DUO single crystal diffractometer in the Debye-Scherrer geometry by the procedure described in [34]. The powder X-ray diffraction analysis of the obtained diffraction patterns reveals that in the region not irradiated by the proton beam, LiOH, $Li_2(CO_3)$, Li_3N phases are always clearly observed whereas in some particles taken from the region irradiated by the beam these phases were detected along with amorphous particles. A similar result was obtained in the analysis of the lithium surface on a LabRAM HR Evolution Raman spectrometer.

Then lithium was washed off with water and the sample was analyzed on a scanning profilometer with confocal chromatic sensors made in the Institute of Automatics and Electrometry (Novosibirsk, Russia). CL1 MG200 and CL4 MG35 sensors (Still SA, France) were used to measure the sample profile with resolutions of 5.7 and 40 nm, respectively. The sample moving system makes it possible to measure a sample profile on a 200 × 200 mm^2 area with a resolution of 100 nm, a positioning accuracy of ± 0.4 μm, and a reproducibility of ± 0.1 μm. The image of the sample surface is presented in Fig. 6. A distinct dark halo *1* with a thickness of 1 mm and an inner diameter of 13 mm deserves attention – it coincides with the position of the main power of proton beam. In Fig. 6 we can also see the center of target copper disc (2), blisters (*3*) remained on the periphery of the proton beam, and the copper disc surface not irradiated by protons (*4*).

The sample surface profile was measured in a rectangular with a width of 0.7 mm, a length of 84.9 mm with a step of 1 μm; the center of the sample was located near the center of the measurement region. The profile measured along the large side of the rectangular and passing through the center of the sample is shown in Fig. 7. Here the center of the sample is identified by an elevation near the X-axis coordinate of 39,500; the dark halo observed in Fig. 6 is identified by the solid color at coordinates of 35,000 and 50,000.

The absence of the expected deepening of the region subjected to intense irradiation by a proton beam (in Fig. 7 this is the region of abscissa coordinates from 35,000 to 50,000) is the first that should be noted in the measured profile. It is considered that at fluences of 10^{17}–10^{20} cm^{-2} the surface layer is completely or partially detached from the bulk, which corresponds to surface modifications such as blistering and flaking [10]. At fluences above 10^{19} cm^{-2}, which appreciably exceed the critical fluences of the blistering onset, blisters and flakes are removed as a result of sputtering. Therefore, deep layers come out to the surface [10]. According to these considerations, irradiation of the copper surface by protons with a fluence exceeding the fluence of the blistering onset by a factor of 200 should cause

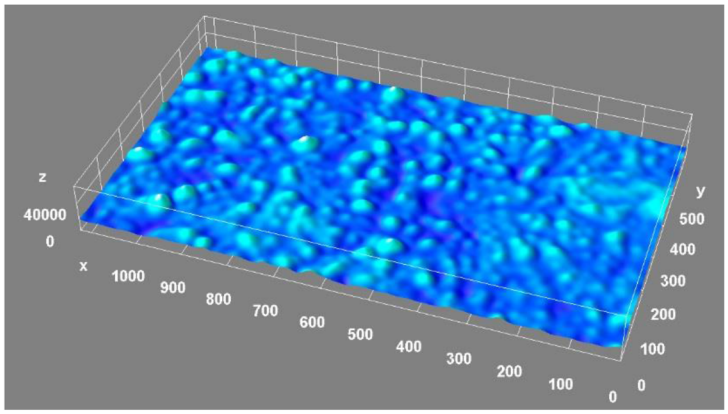

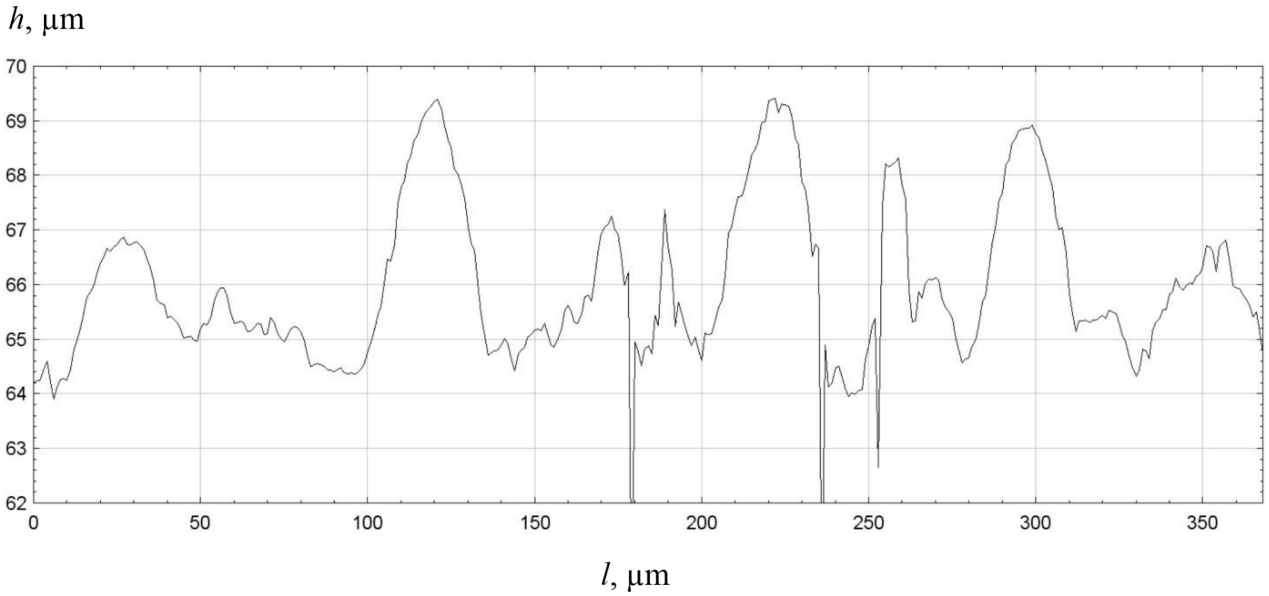

Fig. 13. Copper surface profiles in the region of low-intensity irradiation.

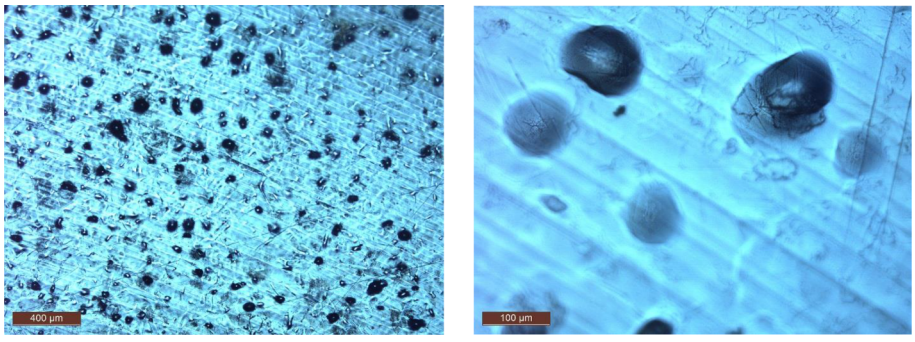

Fig. 14. Image of the copper surface taken on the DM 5000 Leica electron microscope.

significant erosion of metal – a destruction of the metal surface layer as a result of sputtering and flaking. Since the proton penetration depth in copper was 7 μm, then in the region of intense irradiation by the beam a deepening of more than 7 μm should be expected, however, it is not so. The surface copper layer is not removed.

This phenomenon can be explained as follows. Since copper is coated by a thin lithium layer, this layer prevents the removal of blister covers and flakes from this region. Suppose that a 7 μm thick layer detached from copper (as blister covers and flakes) but the lithium layer holds them in place, and this detached layer is still subject to the proton action. A long-term action of high energy protons destructs the crystal bonds in this detached layer and transforms it into the amorphous state. After the completion of irradiation, when lithium was washed off with water, it could be expected that this amorphous layer with a thickness of 7 μm was washed off together with lithium, but this did not happen. As shown below, lithium mixed with amorphous copper and this lithium-copper layer is firmly held on the surface of crystalline copper and provides a good heat capacity.

Let us describe in more detail the results of measuring by the scanning profilometer with confocal chromatic sensors. We move from the center of the target subjected to the intense action of the proton beam to the periphery, up to the non-irradiated surface. Fig. 8 shows the image of the central part of the target and the 2D surface profile. Fig. 9 presents the profile along the line passing through the center of

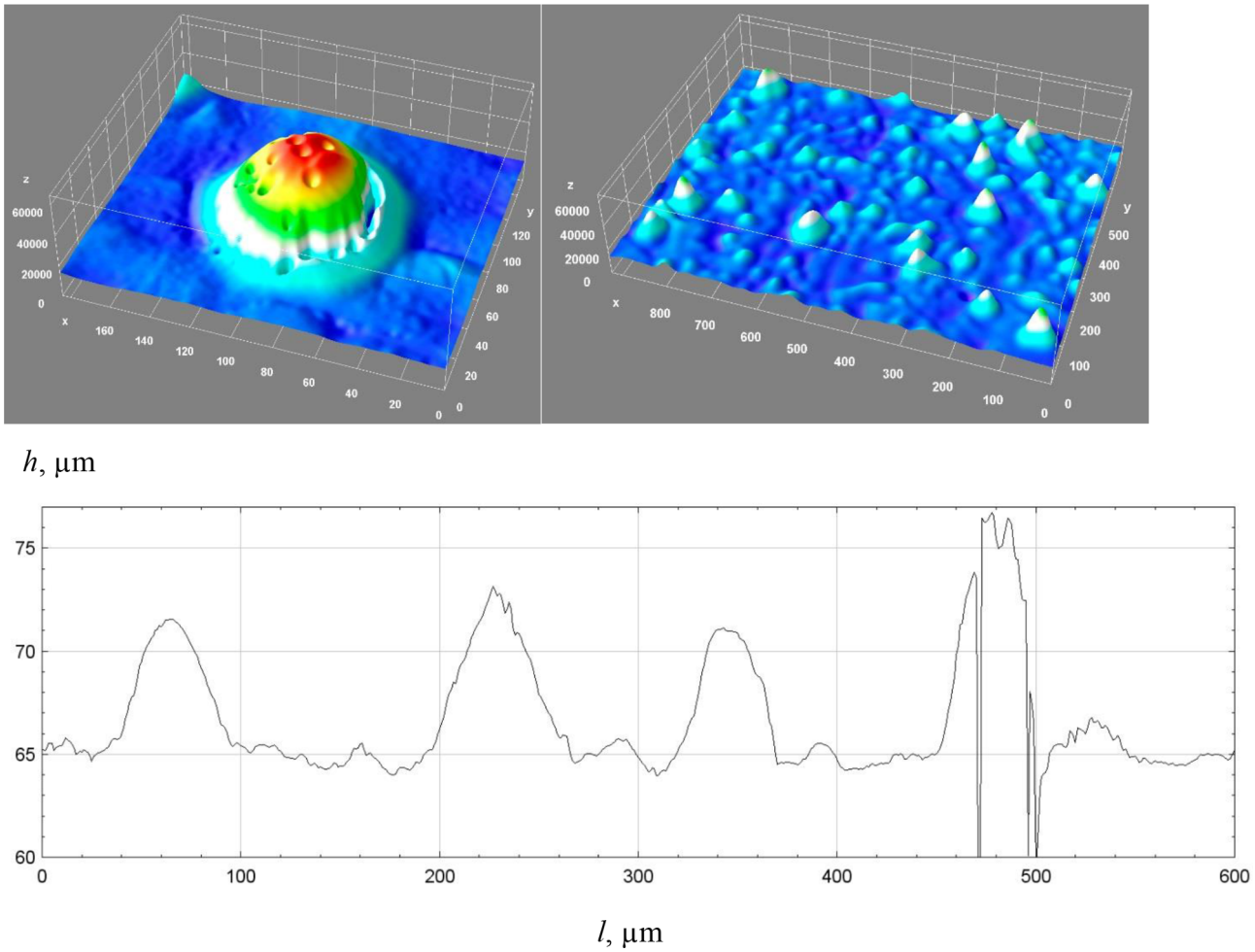

Fig. 15. Copper surface profiles measured on the scanning laser profilometer.

the target. A 3 μm high and 100 μm wide elevation in the center is most likely to be due to the fabrication of the copper disc on a lathe. The same process may be the reason for micron pits spirally diverging from the center of the targets. No blisters or craters are observed inside the dark halo (*1* in Fig. 6).

Surface profiles of the dark halo (*1* in Fig. 6) are depicted in Figs. 10 and 11. In the plot of the surface profile there are many vertical lines indicating the presence of many sharp pits from whose slopes the sent laser beam is not reflected back. It is quite possible that these small-scale pits are generated by thermal breaks due to a high power density gradient. It is most likely, and this is consistent with the measured proton beam size, this halo separates the region of a high proton fluence that is larger than the blistering fluence by factors of tens and hundreds from the region of a low proton fluence comparable with the blistering fluence on the copper surface.

Outside the dark halo, blisters and craters are already clearly seen (in Fig. 7 these are the abscissa coordinate regions from 20,000 to 35,000 and from 50,000 to 65,000). This region was subjected to irradiation by the periphery part of the proton beam with a fluence comparable with the blistering fluence. Craters (Fig. 12) and blisters with a characteristic size of 30 μm (Fig. 13) can be observed closer to the center, farther from the center of the beam the surface is covered by blisters with a height of 5–10 μm and a diameter of about 100 μm (Figs. 14 and 15).

The relief of the copper surface not subjected to irradiation is shown in Fig. 16. The product processing structure with a roughness less than 1 μm is seen.

The composition of water that washed off lithium from the target surface was determined on an atomic emission spectrometers ICPE-9820 (Shimadzu, Japan). In one of the samples with a volume of 5 ml the lithium concentration was 215 ppm and the copper concentration was 0.24 ppm. In another sample, they were 365 ppm and 0.16 ppm, respectively. It is seen that the copper concentration in water is insignificant. This fact evidences that not any significant amount of copper was removed from the target surface when lithium was washed off with water.

We present the main results of series I experiments as follows.

1. As should be expected, 2 MeV proton irradiation of the target in the form of a copper disc coated by a thin lithium layer generates blisters on the copper surface. The blistering fluence and blister sizes correspond to the parameters of previous studies of blistering of the copper surface without lithium [29]. Blisters on the copper surface manifest themselves through the lithium layer as elevations. A decrease in the neutron yield of the ^{7}Li(p,n)^{7}Be reaction due to blistering on the copper surface was not detected.
2. Further proton irradiation of the target causes a gradual disappearance of blisters in the intense irradiation region. Any copper erosion or removal of the surface copper layer are not detected, which may be explained by the presence of a thin lithium layer holding copper flakes that inevitably appear. Since they are not removed, they are subject to further proton irradiation and the copper structure is most likely to transform from crystalline into amorphous one. A decrease in the neutron yield of the ^{7}Li(p,n)^{7}Be reaction due to the copper structure modification is not detected.
3. As a result of long-term proton irradiation of the target through the

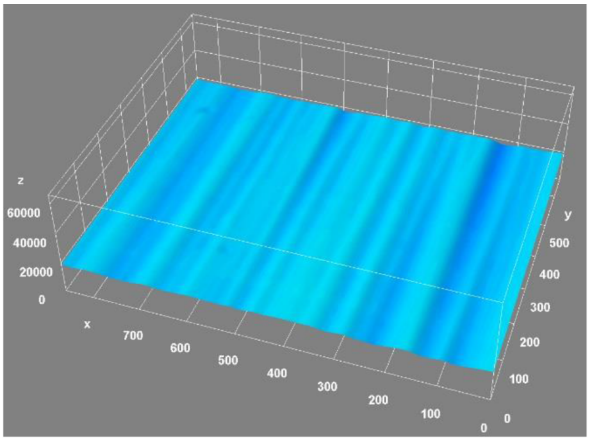

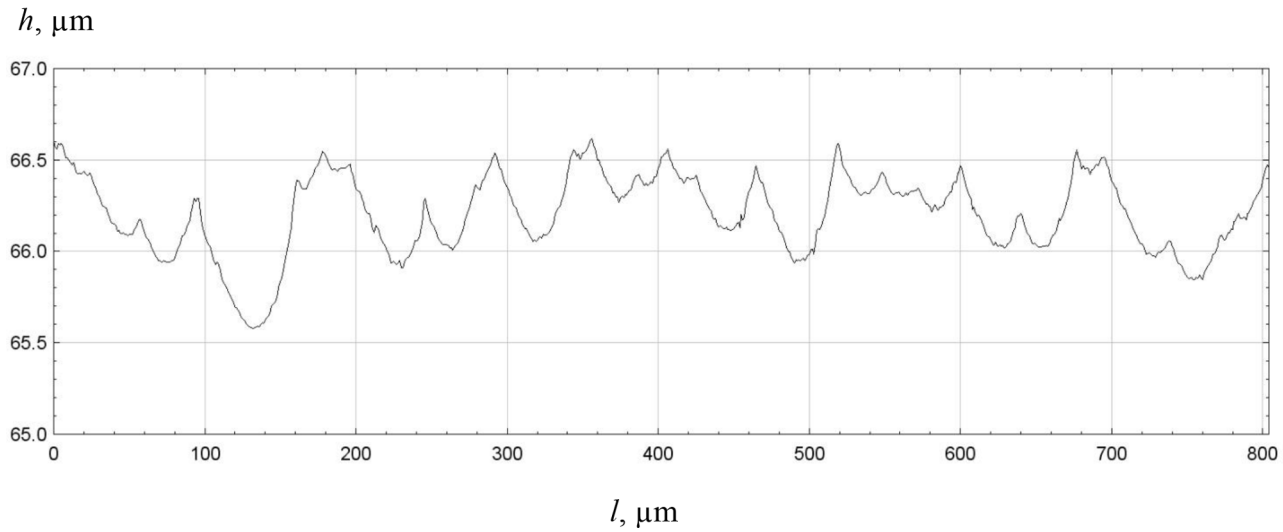

Fig. 16. Profile of the copper surface not subjected to proton irradiation.

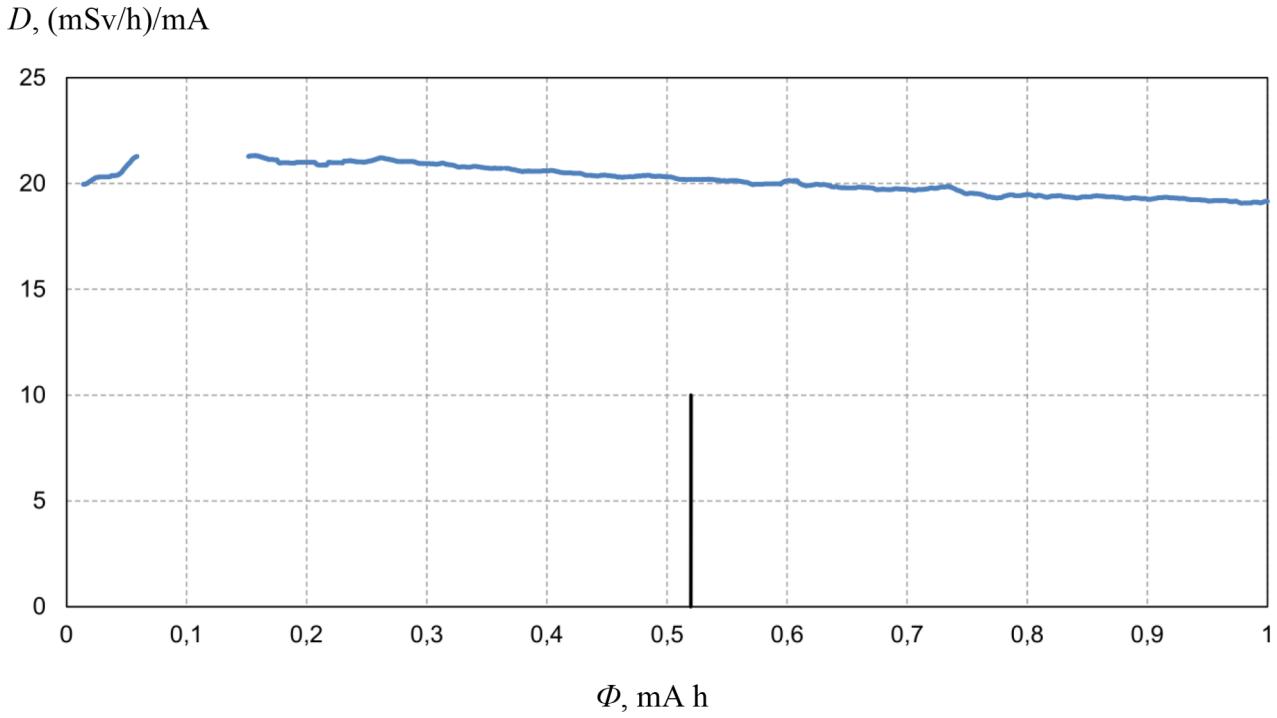

Fig. 17. Dependence of the neutron radiation dose rate D on the proton current integral Φ on the first day of irradiation.

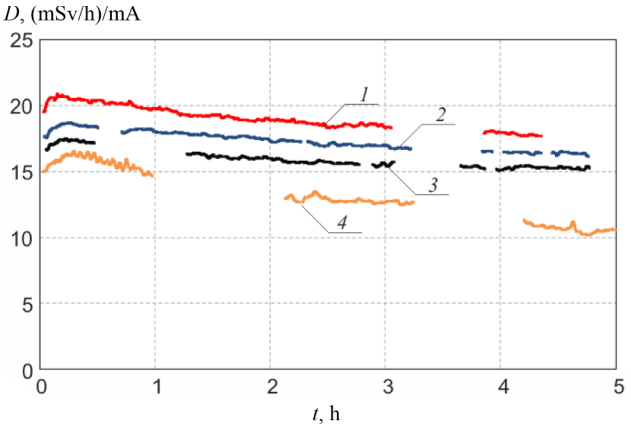

Fig. 18. Time dependence of the signal measured by dosimeter No. 2: *1* – during the second day of irradiation, *2* – on the fourth day, *3* –on the fifth day, *4* – on the sixth day.

lithium layer, the number of passed protons is larger than the number lithium nuclei in the beam size region. In this case, at a lithium thickness of 84 μm and a proton fluence of 6.3 10^{20} cm^{-2} this excess is 1.62. A significant amount of hydrogen was delivered to the near-surface copper layer. As a result of diffusion or through the cracks formed, as noted in [29], this hydrogen reaches lithium. If hydrogen reacted with lithium and formed lithium hydride, then the neutron yield would drop by 30% [31]. A decrease in the yield was not detected, and this means that hydrogen delivered by the proton beam and released from the target does not react with lithium.

3.2. Measurement results and discussion. Series II

In the second series of experiments, a lithium layer with a thickness less than the neutron generation thickness was evaporated on the copper sample.

The sample under study was made from 99.99996% coarse-grained copper (Mitsubishi Materials Co., Tokyo, Japan). The blistering threshold on the surface of this sample was 3.5 times higher than the blistering threshold of the sample used in the first series of experiments [29]. A 9.6 μm thick lithium layer (27 mg of lithium) was evaporated on the sample. The sample was irradiated by a proton beam with a current of (500 ± 10) μA for 4–5 h a day during 7 days. The total accumulated proton fluence was 14.9 mA h.

Unlike the first series of experiments, when the sample was irradiated by a proton beam with a proton energy below the neutron generation threshold and above it for a short time to determine the neutron yield, in the second series of experiments, the sample was irradiated by a proton beam always with a proton energy higher than the neutron generation threshold: usually 2.04 MeV and energies ranging from 1.9 to 2.17 MeV for a short time to measure the neutron yield.

In the second series of experiments, we specially used copper more resistant to blistering in order to more reliably compare the neutron yield before and after blistering on the first day of irradiation. Fig. 17 shows the dependence of the neutron yield measured by dosimeter No. 2 and normalized to the proton current on the accumulated proton fluence (the absence of the signal in plots in Figs. 17 and 18 is explained by calibration – at these points of time the proton energy was altered). The blistering threshold was 0.52 mA h in this copper sample (shown by a vertical line in Fig. 17). No abrupt change in the neutron yield is observed in the transition region through the blistering threshold.

The time dependence of the dose measured by dosimeter No. 2 in other days of irradiation is depicted in Fig. 18. It is seen that the measured signal decreases during the day and decreases day by day. During the first four days the signal decreases on average by 14%, out of which 11.5% are due to a decrease in the proton energy by 0.65% because of heating of the resistor voltage divider (noted in the section "Features of measurements") and 2.5% are due to actual neutron yield

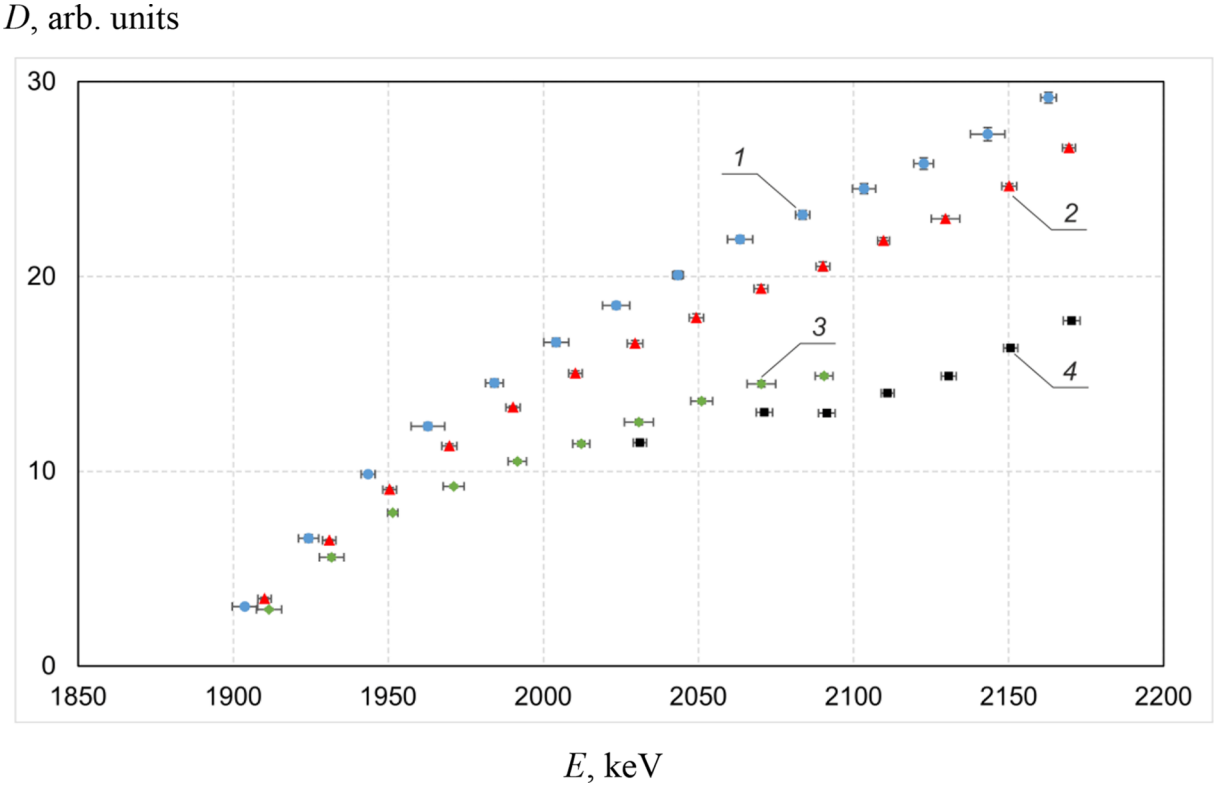

Fig. 19. Dependence of the neutron radiation dose rate measured by dosimeter No. 2 on the proton energy *E* on different days of irradiation: *1* – the first day, *2* – the fourth day, *3* – the sixth day, *4* – the seventh day.

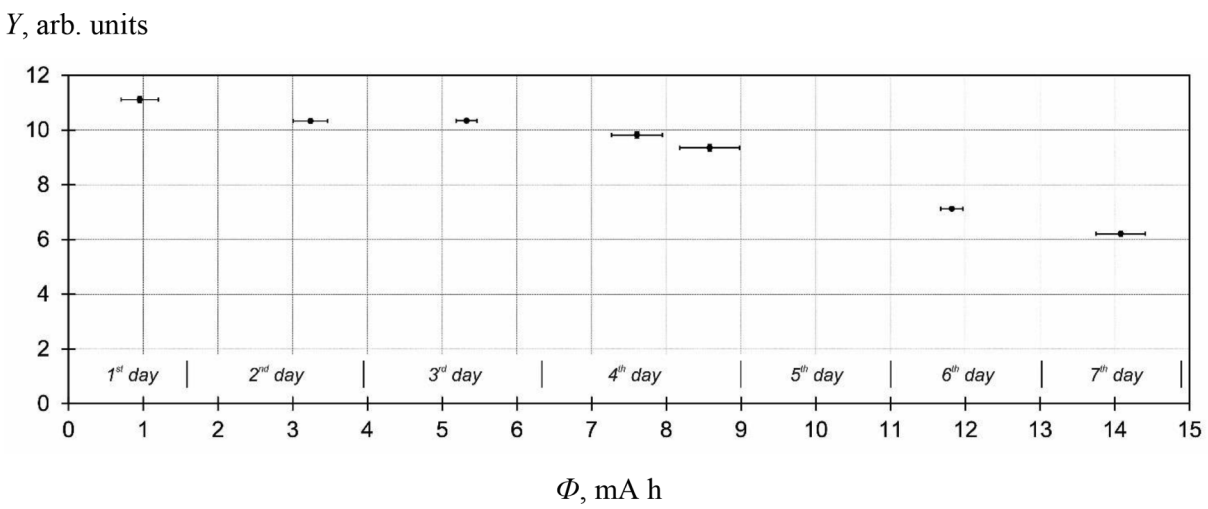

Fig. 20. Dependence of the neutron yield Y measured by dosimeter No. 2 on the accumulated proton current integral Φ.

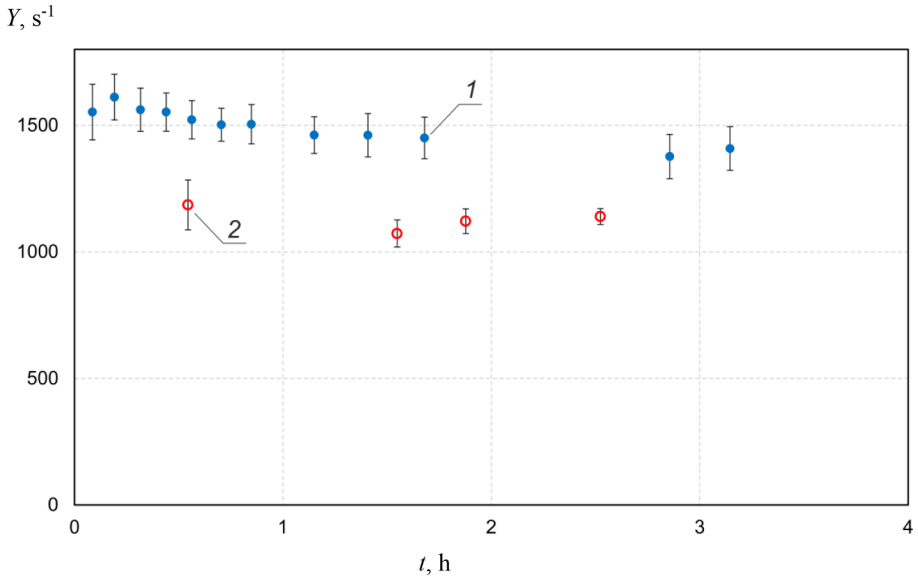

Fig. 21. Time dependence of the average count rate of the neutron detector on the first (*1*) and seventh (*2*) days of irradiation.

degradation.

Neutron yield degradation is most likely to be caused by lithium penetration into copper. The lithium layer thickness diminishes and the neutron yield from it becomes less. Then protons start to slow down in copper, and of course, can interact with lithium penetrated into copper, however, the proton energy can already be insufficient to generate neutrons.

Fig. 19 illustrates the results of the performed measurements of the dependence of the neutron yield on the proton energy which enable the energy calibration by the neutron generation threshold and the accurate measurement of the neutron yield. Here we can also see degradation of the neutron yield with time. Figs. 20 and 21 show the dependence of the neutron yield on the accumulated proton fluence.

Generalizing the results of the performed study, it is possible to state the following. During the first four days of irradiation the neutron yield evenly decreased by (2.5 ± 1) % per day, and in total, it decreased by (10 ± 1) % to a (90 ± 1) % level from the initial one in four days. During the fifth day the neutron yield degradation rate increased to (5 ± 1)% per day, and over the next two days the degradation rate increased even more – to (10 ± 2) % per day. To the end of irradiation of the target (in seven days) the neutron yield was (63 ± 3) % from the initial one.

Neutron generation as a result of the $^{7}Li(p,n)^{7}Be$ reaction is known to be accompanied by the accumulation of a radioactive beryllium-7 isotope emitting gamma-rays with an energy of 478 keV and a half-life of 53 days in the lithium layer. It might be expected that the washing-off of lithium with water would lead to deactivation of the target, but this did not fully happen. The count rate of this radiation line measured by a SEG-1KP-IFTP gamma-ray spectrometer based on a semiconductor detector made from high-purity germanium decreased to a 10% level from the initial one. It is most probable that lithium together with beryllium formed penetrated into copper and was not washed off with water.

We present the main results of series II experiments as follows:

1. The appearance of blisters on the copper surface does not cause changes in the neutron yield.
2. Constant degradation of the neutron yield from the lithium target was experimentally measured at a lithium thickness less than the neutron generation thickness.
3. The penetration of the radioactive ^{7}Be isotope formed into the copper disc, more precisely, into the layer not washed off with water was experimentally stated.
4. It is assumed that neutron yield degradation is caused by lithium

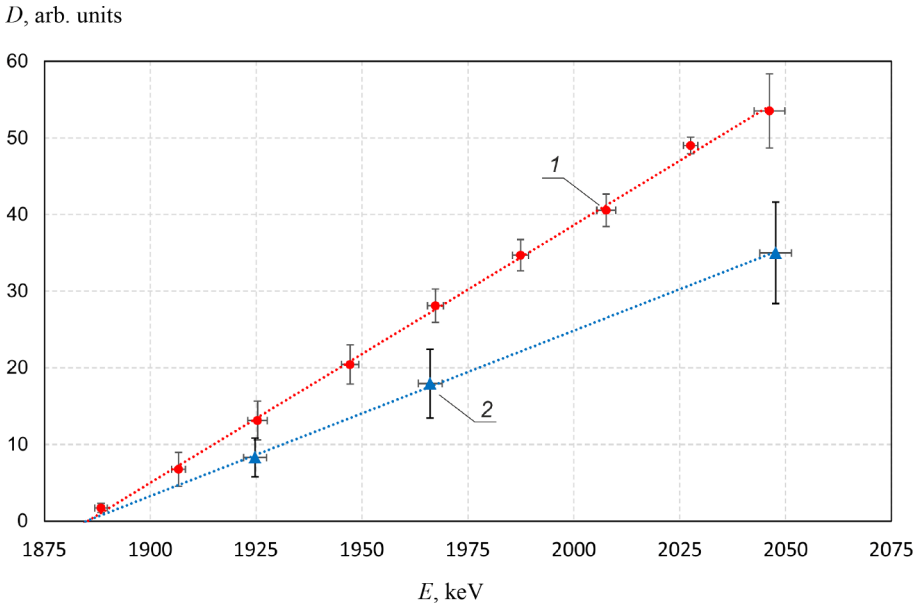

Fig. 22. Dependence of the neutron radiation dose rate D on the proton energy E for two proton beam fluences: *1* – 1.9 mA h, *2* – 8.5 mA h.

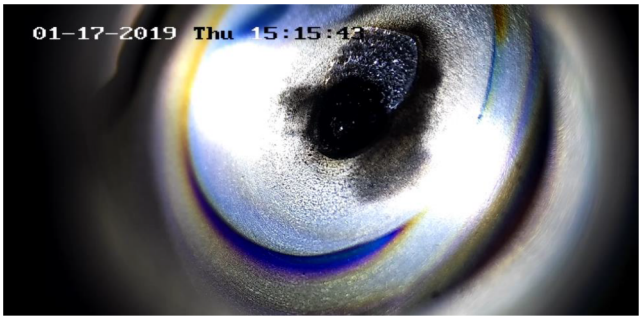

Fig. 23. Image from the video camera. The proton beam impact area is located closer to the center.

penetration into copper, as a result of which, protons with an energy exceeding the neutron generation threshold begin to slow down more on copper and less interact with lithium.

3.3. Measurement results and discussion. Series III

In the third series of experiments, the sample was made from 99.99% copper (Mansfelder Kupfer und Messing GmbH, Germany). A 68 μm thick lithium layer was evaporated on the sample (189 mg of lithium). The sample was continuously irradiated by a 2 MeV proton beam with a current from 1 to 3 mA for 4 h.

At first, the proton beam was 1 mA. After the proton fluence of 1.9 mA h was accumulated, the dependence of the neutron radiation dose rate on the proton energy was measured. The result is illustrated in Fig. 22. Then the proton beam current was increased to 3 mA and we observed that at such a high heating power (8 kW/cm^2) lithium became liquid under the proton beam but it did not sink anywhere (Fig. 23). After the fluence of 8.5 mA h was accumulated, the dependence of the neutron dose rate on the proton energy was measured again. In Fig. 22 it is seen that the neutron yield dropped by 36%, although the lithium layer thickness significantly exceeds the neutron generation thickness.

After irradiation the target was removed and lithium was washed off with water. The water conductivity was measured by a PHT-028 Multi-parameter Water Quality Monitor (Shenzhen Handsome Technology Co., Ltd.) and the lithium concentration was determined in it. It was 171.6 mg whereas 189 mg were evaporated. From here it follows that 9.2% of lithium remained on the target, which is consistent with the prediction of the possible penetration of lithium into copper, which was made in the formulation of the main results of the previous series of experiments.

Photos of the target with lithium before and after irradiation and after lithium was washed off are presented in Fig. 24. Note good homogeneity of the evaporated lithium layer (a), exfoliation of the lithium layer on the periphery after irradiation (b), and appreciable copper erosion in the proton beam area (c).

After lithium was washed off, the sample was analyzed on the scanning profilometer with confocal chromatic sensors. The image of the surface under study and the measured profile are shown in Fig. 25. It is seen that the copper surface was subjected to significant erosion: craters with a size up to 3 mm and a depth up to 0.2 mm are observed.

Then two samples with dimensions of 7 × 7 × 8 mm were cut by the electric spark linear cutting machine from the copper disc (Fig. 26a). The prepared samples were pressed into polymer resin on a Buehler Simplimet 1000 instrument. Cut surfaces were smoothed and polished on an automated machine with gradually decreasing size of abrasive particles from 60 μm up to 3 μm. The final polishing was made with the use of colloidal silicon oxide with a particle size of 0.05 μm. Fig. 26b shows the photos of samples in the polymer form which were prepared for microscopic examinations.

The microstructure of the samples was observed on an EVO 50 XVP scanning electron microscope (Zeiss, Germany) in two modes: i) SE when the image is obtained by knocking out secondary electrons from the samples, and this mode provides information on the releif; ii) BSD when the image is obtained by back-scattered electrons, and this mode makes it possible to reveal differences in the composition of the sample under study (regions with a prevailing concentration of lighter elements are darker in the image than regions with heavier elements). To analyze the elemental composition by X-ray spectroscopy an x-ACT SDD detector (Oxford Instruments, GB) was used. The samples were irradiated by a 20 keV picoampere electron beam.

We present two images from many of them. Fig. 27 is a characteristic image of a microjunction of two samples. The boundary line of the samples is in the center of the images. The proton beam falls on the surfaces from the boundary line toward each sample. The area perpendicular to the proton beam is examined. Fig. 27a shows the general view of the junction, and in Fig. 27b the junction region is magnified. It is distinctly seen that a layer formed from the surface into the sample

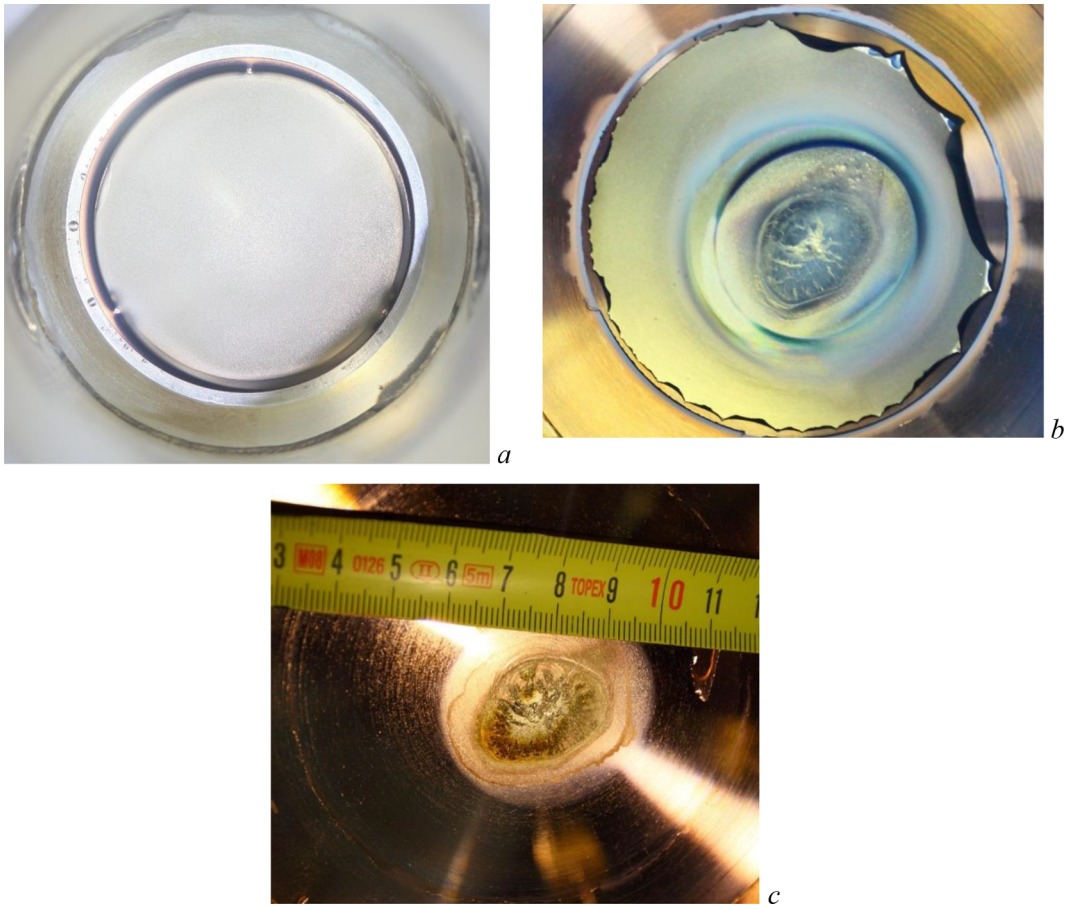

Fig. 24. Photos of the target before (a) and after (b) irradiation and after lithium was washed off (c).

bulk, which looks darker than the main material of the sample. The layer thickness is around 35 μm in each sample. Since the proton penetration depth into copper is less than 7 μm, it is possible to state that the copper surface with a thickness exceeding the proton path length is modified.

Fig. 28 shows the images of regions with maximum erosion. The features of this image are that i) the only one sample is seen in it because between the samples there was a free space; ii) not only a cut is seen but also the surface subject to proton irradiation and not subject to any treatment, including polishing. This layer with a thickness of about 15 μm is seen in Fig. 28*a* as flakes between the light image of the treated cut of the sample and a dark image of the free space. After taking this image, the sample was etched by a 50% nitric acid solution and the same region was again observed. In Fig. 28*b* it is seen that this layer of flakes disappeared after etching. It is most probable that we managed to obtain the image of copper layers (flakes) detached from the copper sample as a result of blistering and not mixed with lithium penetrated into copper (Fig. 28a)

The X-ray spectroscopy analysis of the elemental composition of different layers of the samples made it possible to determine copper, oxygen, and carbon contents in them but not lithium because its characteristic radiation is 40 eV and lies in the low energy range, which is not reliably measured by the detector. Fig. 29 displays an image of the sample with indicating the place of the spectral measurement and the measured spectrum. In the modified region with a thickness of about 35 μm (it is located between lighter and darker parts), the weight content of copper ranges from 92 to 94%, of carbon from 3 to 5%, oxygen from 1.5 to 2%, silicon from 0.4 to 0.6%. The presence of silicon and carbon is explained by the specific features of sample treatment. In the region not subject to modification (left in the figure), the weight content of copper ranges from 95.5 to 96%, of carbon from 2.2 to 2.4%, oxygen from 1.4 to 1.5%, silicon from 0.5 to 0.6%. It can be said for sure only the copper layer subject to modification is more porous than that not subject to modification.

In the course of measurements of the sample surfaces, we detected micron spots or bubbles whose nature was not revealed. Fig. 30 shows the surface images taken in two modes of the electron microscope. Since the images do not significantly differ from each other, the conclusion may be drawn that the observed features are the surface relief rather than chemical compounds.

To determine the phase composition of the target region subjected to intense proton beam irradiation, an X-ray study was carried out. A particle of about 0.5 mm was cut (using a scalpel) from the center of the target from the region of intense proton irradiation (Fig. 26a, lower right corner of the square). Its study was carried out in the Debye-Scherrer scheme on a Bruker D8 Venture X-ray diffractometer (Incoteac 1 S 3.0 microfocus tube, CuKα radiation, three-circle goniometer, PHOTON 3 detector, resolution 768 × 1024, pixel size − 135 μm). Si-SRM640 silicon (a = 5.4309 Å) was used as a standard. X-ray phase analysis (Fig. 31) showed that, in addition to reflections of the main phase based on a face-centered close-packed Cu lattice (reflex indices are shown in Fig. 31), there are a number of low-intensity reflections, which are attributed to Cu_2O and LiO_2. A detailed analysis of the profiles of the main reflections showed the presence of satellites from the side of large angles 2Θ. The inset in Fig. 31 shows a profile of a reflex 220 that can be decomposed into two components. This indicates that the sample contains two fcc phases with close values of the unit cell parameters: 3.645(2) and 3.615(2) Å. The second value, within the experimental error, coincides with the theoretical value for Cu (a = 3.6149 Å). The phase with an increased value of the unit cell parameter can be associated with the formation of a solid solution of

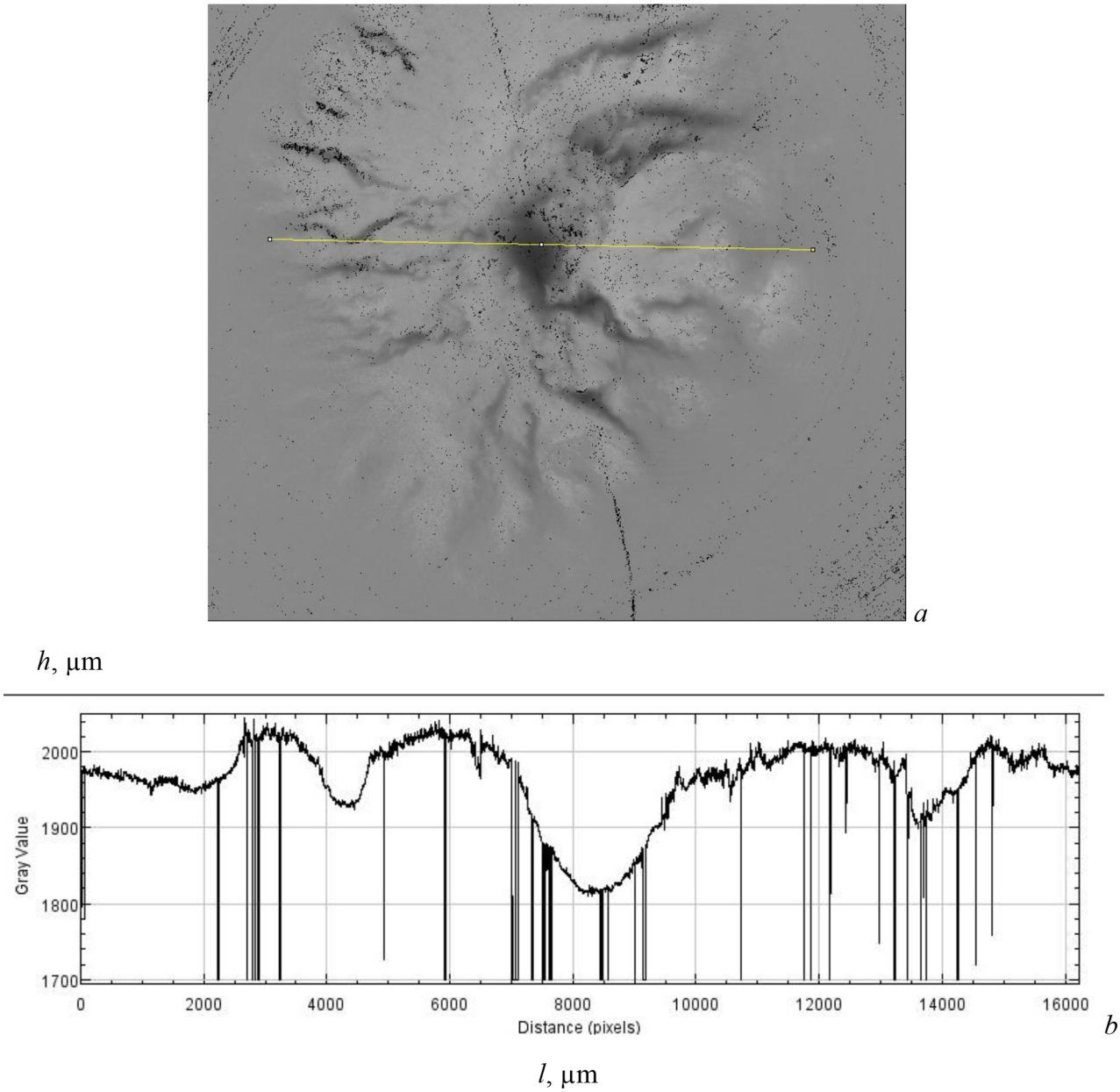

Fig. 25. Image of the copper surface with a profile measurement line (*a*) and the measured profile (*b*).

the introduction of lithium atoms into the crystal structure of copper - Cu(Li). According to the data of [35], in which the dependence of the unit cell parameter of Cu on the number of intercalated lithium atoms was studied, the value we measured corresponds to approximately 18% Li.

We present the main results of series III experiments as follows:

1. At a high proton beam power density lithium evaporated on copper becomes liquid but does not drain.
2. Despite that the lithium thickness is larger than the neutron generation thickness, neutron yield degradation is observed during irradiation.
3. Intense proton irradiation causes substantial copper erosion, and possibly, lithium penetration deeper than the proton stop. The active interaction between copper and lithium was noted in [36].
4. The image of the layer was taken, which most likely consisted of copper flakes exfoliated from the copper sample as a result of blistering and lithium. This layer was not washed with water but was removed by etching.

3.4. Measurement results and discussion. Series IV

The aim of the fourth series of experiments was to reveal whether lithium penetrated into copper during evaporation in a vacuum or proton irradiation before blistering or only during proton irradiation after blistering.

The experiment was performed in somewhat another geometry to decrease the proton beam current density and have the possibility to irradiate the target for a noticeable time until blistering. The target was made from 99.996% pure copper, placed in the vertical part of the proton beam transport line after the bending magnet and the magnetic scanner – where it is usually located during biological studies [4,5]. At this placement of the target, dosimeter No. 2 (*8* in Fig. 1) turned out to be at a distance of 6.4 m from the target at an angle of 136° to the proton beam direction. The target was irradiated by the proton beam with a diameter of 4 cm, the current of 1 mA, and the energy of 1.85 to

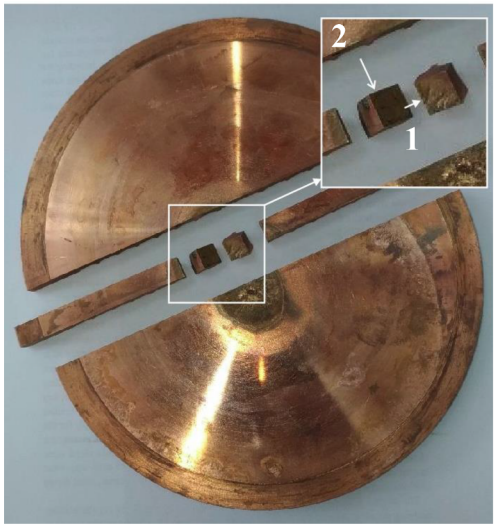

а

б

Fig. 26. *a* – Photo of the substrate of the neutron-generating target cut to prepare samples. Arrows indicate sample faces that were later subjected to polishing and they were in the observation plane during microscopic studies. *b* – Photo of the samples in the polymer form with the polished face oriented to the observer. Digits in the figure (*a*) correspond to digits in the figure (*b*).

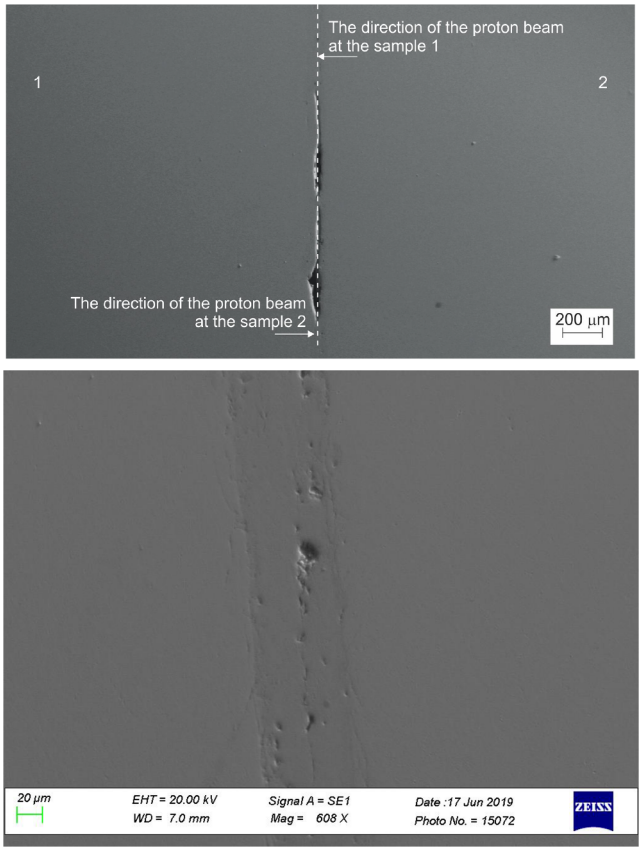

Fig. 27. Image of the sample junction.

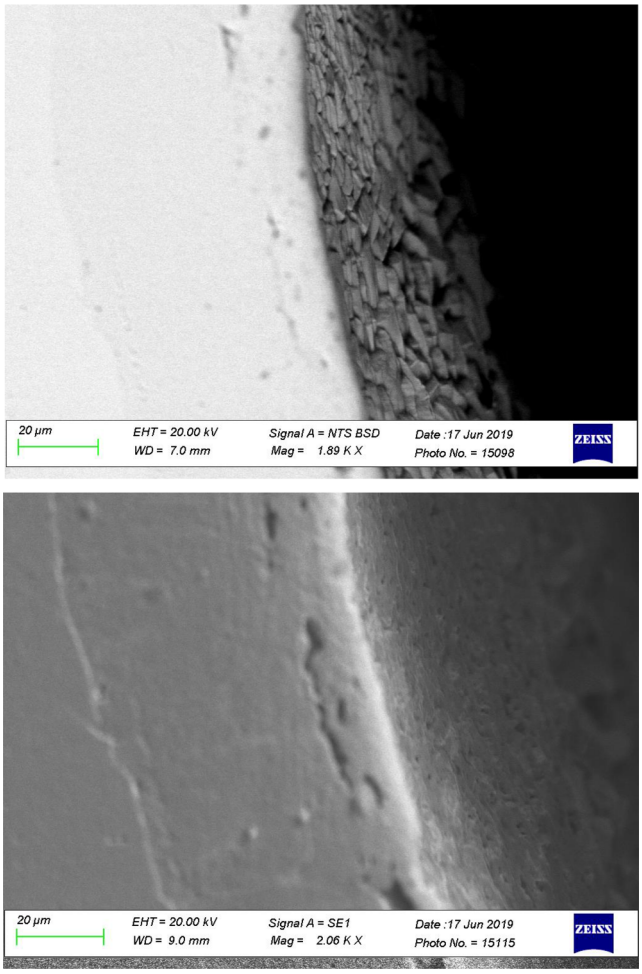

Fig. 28. Image of the region with maximum erosion.

2.25 MeV for 40 min. At the accumulated current integral of 0.66 mA h and the beam diameter of 4 cm the maximum proton fluence was 1.15 10^{18} cm^{-2}, which is almost four times less than the blistering threshold [29].

At first, we irradiated two similar targets with a 1 µm thick lithium layer with the only difference that the lithium layer was washed away with water from the second target before irradiation. Fig. 32 illustrates the dependence of the neutron dose rate measured by the dosimeter on the proton energy during irradiation of these two samples, with the measured signal from the target without the lithium layer being magnified 500 times for the convenience of comparison. The neutron yield from the target from whose surface lithium was washed off with water is observed to be 700 times less. This fact indicates that during lithium evaporating in a vacuum on the air-cooled copper disc, no noticeable penetration of lithium into copper occurs. It is worth paying attention to Fig. 24b in which it is seen that after irradiation of the

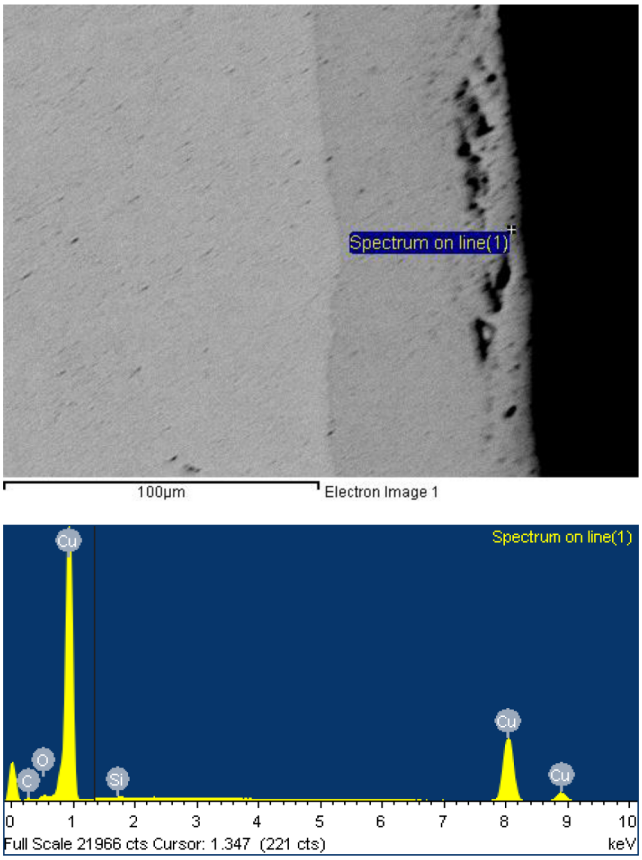

Fig. 29. X-ray spectroscopy analysis: *a* is the sample cut with indicating the point for which the spectrum was measured; *b* is the X-ray spectrum (*x* axis is the X-ray energy of the sample in keV, *y* axis is the X-ray intensity.

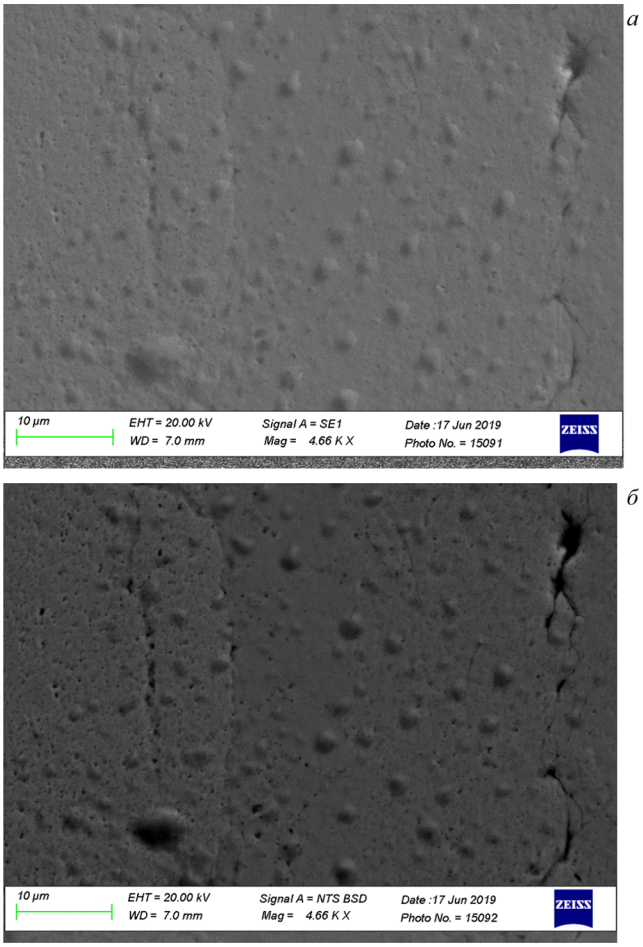

Fig. 30. Images of the same region taken in different modes of the microscope electron beam: (a) secondary electrons (SE), (b) back-scattered electrons (BSD).

target the lithium layer on the periphery detached from the copper substrate, which evidences poor adhesion between lithium and copper.

Then the target with the 10 µm thick lithium layer was irradiated. After irradiation the target was taken out and placed into the developed γ-spectrometry complex consisting of a SEG-1KP-IFTP γ-spectrometer based on a semiconductor detector made from high-purity germanium, 50 mm thick lead collimator with a 2.5 mm hole and a 2D movable controlled desk. Fig. 33 presents the control program screenshot with the measurement result. It is seen that a 40 mm region emits 478 keV gamma rays as a result of decay of ^{7}Be nuclei formed in the ^{7}Li(p,n)^{7}Be reaction. This region coincides with the proton beam size and location on the target.

Then lithium was washed off with water and by means of two techniques it was found that one third of lithium amount remained in copper. The conductivity measurement of water with which lithium was washed away indicates that it contained 22 mg of lithium whereas we evaporated 30 mg. The DSC-96 dosimeter-radiometer with a BDMG-96 detection unit (Dose, Russia) measured the γ-ray dose rate of the target of 40 µSv/h, which was due to the accumulation of the ^{7}Be radioactive isotope after lithium was washed with water whereas it was 120 µSv/h before the washing. This result indicates that 3 µm of lithium penetrated into copper.

Lithium penetration into copper was also confirmed by the following. After proton irradiation of the target with the lithium thickness of 30 µm, the target was taken out and its activation was immediately measured by the SEG-1KP-IFTP γ-ray spectrometer based on the semiconductor detector. In the radiation spectrum two bright lines were detected: with the energy of 478 keV due to the decay of ^{7}Be nuclei formed with the half-life of 53 days and the energy of 511 keV due to neutron activation of copper (^{64}Cu half-life is 12 h). After lithium was

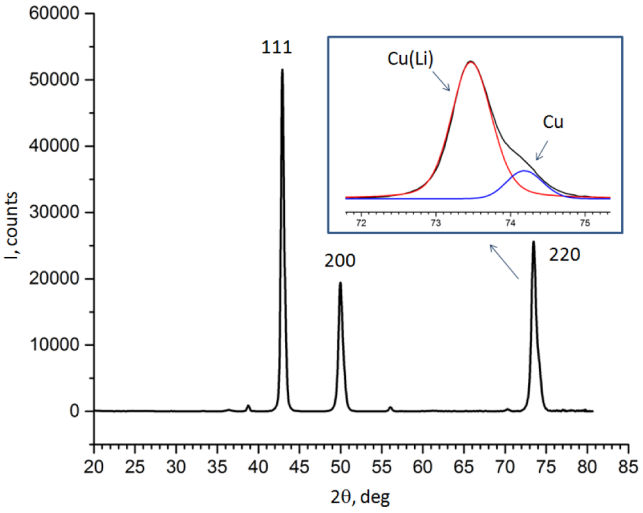

Fig. 31. Diffraction pattern (CuKα radiation) of a target surface area. The inset shows the decomposition of the 220 reflection profile into two components.

washed away with water the 478 keV line intensity decreased by a factor of 12, from 420 to 34 s^{-1} while the 511 keV line intensity remained the same: 41 s^{-1}.

Thus, in the IV series experiments it is found that lithium does not penetrate into copper during evaporating in a vacuum, however, it penetrates during proton irradiation until blisters appear on the copper

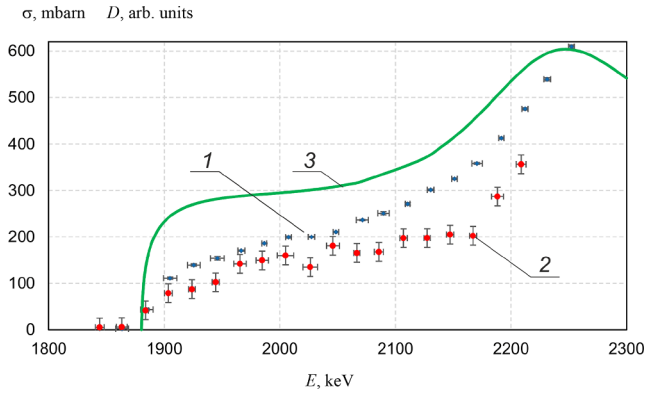

Fig. 32. Dependence of the neutron irradiation dose rate D on the proton energy during irradiation of the target with a 1 μm thick lithium layer (*1*, blue rhombuses) and the target with the lithium layer previously washed away (*2*, red circles; values magnified by 500). The dependence of the ^{7}Li(p,n)^{7}Be reaction cross-section on the proton energy (*3*, green solid line) is given for reference.

surface, which seems to be due to heating.

4. Conclusions

Boron neutron capture therapy needing an intense epithermal neutron beam is a promising technique to treat tumors. It has been generally accepted that neutron generation as a result of ^{7}Li(p,n)^{7}Be and ^{9}Be(p,n)^{10}B threshold reactions at a proton energy in the range 2–3 MeV enables the formation of a neutron beam most satisfying the BNCT requirements. Neutron-generating targets are prepared, as a rule, with three layers: a thin lithium or beryllium layer for neutron generation; a thin metal layer for proton absorption; and an intensely cooled, heat removing copper substrate. The target operation time is considered to be limited by radiation blistering: a deformation process of the metal surface layer expressed as the formation of numerous bulges in the form of lifting and peeling of a thin layer of the material (blisters) under ion bombardment. It is the reason why tantalum or palladium that are most resistant to blistering are used as the second layer of the target.

In this work, we have studied for the first time the effect of copper blistering on the neutron yield from the target made as an intensely

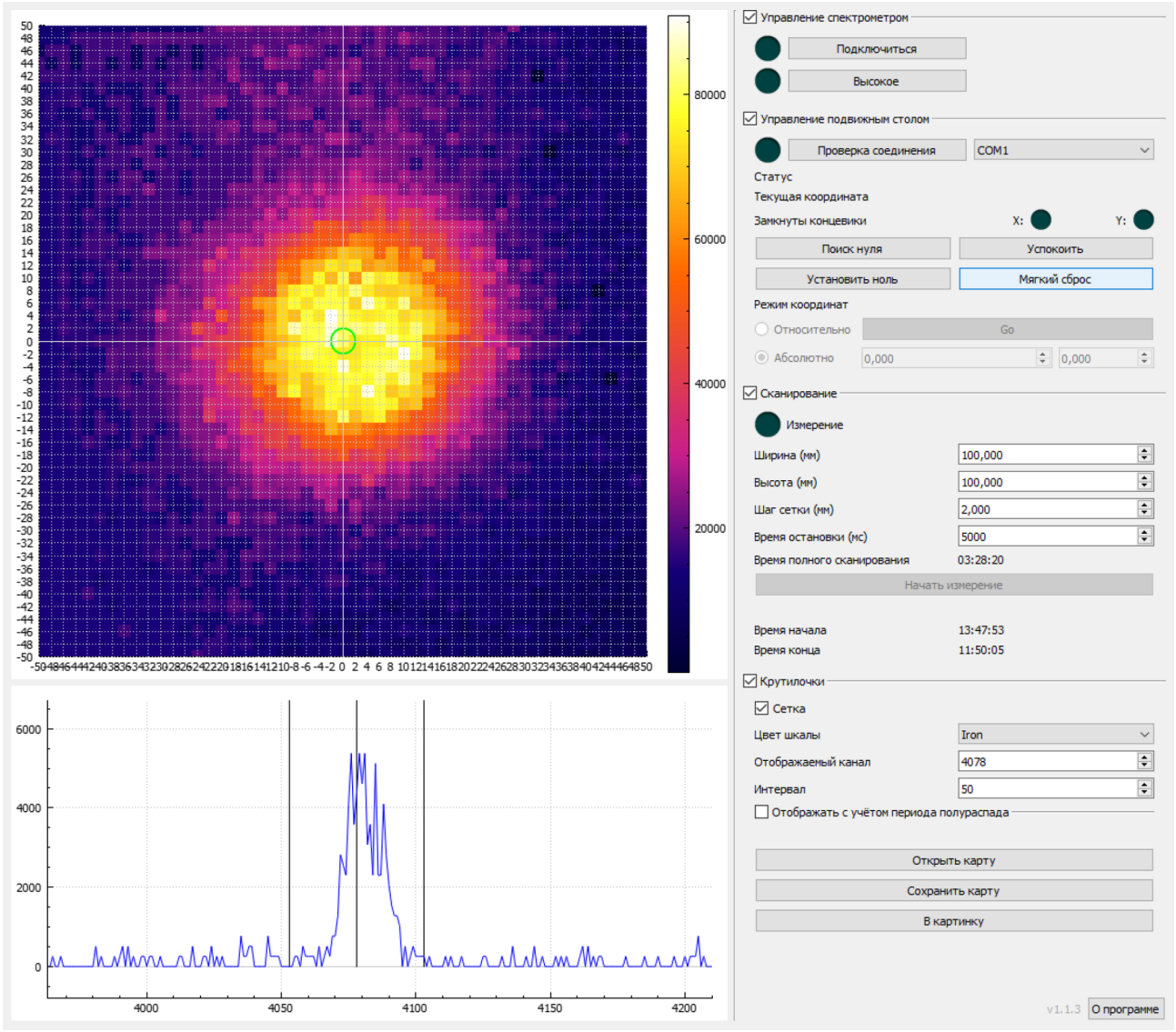

Fig. 33. Control program screenshot of the γ-spectrometry complex with the measurement result of the spatial intensity distribution of 478 keV γ-rays; measurement step 2 mm, point measurement time 5 s.

cooled copper disc with a thin lithium layer evaporated in a vacuum. The experiments were conducted on a vacuum-insulated tandem accelerator providing a proton beam with the energy ranging from 1.8 to 2.2 MeV, the current of 0.5 to 3 mA, and the diameter of 1 to 4 cm.

Two targets were irradiated by the proton beam with a power density of 1.3 kW/cm^2 for a long time. The target made from 99.996% copper with a lithium thickness of 84 μm exceeding the neutron generation thickness was irradiated to a fluence of 6.3 10^{20} cm^{-2} that 200 times larger than the blistering threshold on the copper surface. The target made of 99.99996% coarse-grained copper with a lithium thickness less than 9.6 μm, below neutron generation thickness was irradiated to a fluence of 4.3 10^{20} cm^{-2} that 29 times larger than the blistering threshold. The target with a lithium thickness of 68 μm was irradiated by the proton beam with a power density of 8 kW/cm^2. The targets with lithium thicknesses of 1 and 10 μm were irradiated by a proton beam with a power density of 0.16 kW/cm^2.

During irradiation we performed the *in-situ* observation of the sample surface by virtue of the KX InfiniMax™ long-distance microscope and the Hikvision video camera. The temperature on the surface was measured by a FLIR T650sc infrared camera, the neutron radiation dose rate was measured by two dosimeters, and the neutron flux density was measured by the neutron detector with a lithium-containing scintillator.

After irradiation the samples were analyzed on the LabRAM HR Evolution Raman spectrometer (HORIBA Scientific), the Kappa APEX DUO single crystal diffractometer (Bruker, Germany), the DM 5000 electron microscope (Leica, Germany), the scanning profilometer with confocal chromatic sensors, the EVO 50 XVP scanning electron microscope (Zeiss, Germany), and the ICPE-9820 parallel inductively coupled plasma atomic emission spectrometer with axial and radial plasma viewing (Shimadzu, Japan).

As a result of the experiments performed, we established the following.

1. 2 MeV proton irradiation of the target made in the form of a copper disc on which a thin lithium layer was evaporated in a vacuum, as should be expected, causes blistering on the copper surface. The blistering fluence and blister sizes correspond to the parameters of the previous studies of blistering on the copper surface without lithium. Blisters on the copper surface manifest themselves through the lithium layer as elevations. Their appearance on the copper surface does not change the neutron yield.
2. Further proton irradiation of the target leads to a gradual disappearance of blisters on the region of intense irradiation. No copper erosion or removal of the surface copper layer were detected, which was explained by the presence of a thin lithium layer retaining copper flakes that inevitably appeared. Since they are not removed anywhere, they undergo further proton irradiation and the copper structure becomes amorphous instead of crystalline. A decrease in the neutron yield in the ^{7}Li(p,n)^{7}Be reaction due to the copper structure modification was not detected.
3. When the lithium thickness is less than the neutron generation thickness, degradation of the neutron yield from the lithium target was experimentally detected. This degradation is found to be caused by lithium penetration into copper. It begins when the target is heated by the proton beam, including until blisters appear, and improves the adhesion between the lithium layer and the copper surface.
4. Hydrogen delivered by the proton beam to the near-surface copper layer does not chemically react with lithium, which could result in a drop of the neutron yield.

The obtained results change the existing view on the blistering effect. We have established for the first time that radiation blistering on the copper surface of the lithium target does not lead to neutron yield degradation, i.e., does not make the target inapplicable for exploitation and does not limit its operation time. Neutron yield degradation is possible due to lithium diffusion into copper and can be eliminated by evaporating a lithium layer with a thickness exceeding the neutron generation thickness.

The results obtained are important not only for BNCT, but also for the design of elements of charged particle accelerators and the first wall of a thermonuclear reactor.

Funding

This work was supported by the Russian Science Foundation (grant number 19–72-30005); the TAE Technologies, Inc., CA, USA (the target unit provision).

Data availability

The theoretical and experimental data presented in this work are available from the corresponding authors on reasonable request.

CRediT authorship contribution statement

Timofey Bykov: Visualization. **Nikolay Goloshevskii:** Formal analysis. **Sergey Gromilov:** Validation. **Dmitrii Kasatov:** Investigation. **Yaroslav Kolesnikov:** Formal analysis. **Aleksey Koshkarev:** Software. **Aleksandr Makarov:** Investigation. **Aleksey Ruktuev:** Formal analysis. **Ivan Shchudlo:** Investigation. **Evgeniia Sokolova:** Investigation, Writing - original draft. **Sergey Taskaev:** Conceptualization, Writing - review & editing.

Declaration of Competing Interest

The authors declare that they have no known competing financial interests or personal relationships that could have appeared to influence the work reported in this paper.

References

[1] W. Sauerwein, A. Wittig, R. Moss, Y. Nakagawa (Eds.), Neutron Capture Therapy: Principles and Applications, Springer, 2012. doi:10.1007/978-3-642-31334-9.
[2] S. Taskaev, V. Kanygin, Boron neutron capture therapy, Novosibirsk: Siberian Branch Russ. Acad. Sci., 2016.
[3] B. Bayanov, et al., Accelerator based neutron source for the neutron-capture and fast neutron therapy at hospital, Nucl. Instrum. Meth. A 413 (1998) 397–426, https://doi.org/10.1088/1742-6596/41/1/051.
[4] S. Taskaev, Accelerator based epithermal neutron source, Phys. Part. Nuclei 46 (2015) 956–990, https://doi.org/10.1134/S1063779615060064.
[5] S. Taskaev, Development of an accelerator-based epithermal neutron source for boron neutron capture therapy, Phys. Part. Nuclei 50 (2019) 569–575, https://doi.org/10.1134/S1063779619050228.
[6] B. Bayanov, V. Belov, V. Kindyuk, E. Oparin, S. Taskaev, Lithium neutron producing target for BINP accelerator-based neutron source, Appl. Radiat. Isotopes 61 (2004) 817–821, https://doi.org/10.1016/j.apradiso.2004.05.032.
[7] B. Bayanov, V. Belov, S. Taskaev, Neutron producing target for accelerator based neutron capture therapy, J. Phys.: Conf. Series 41 (2006) 460–465, https://doi.org/10.1088/1742-6596/41/1/051.
[8] D. Kasatov, A. Makarov, I. Shchudlo, S. Taskaev, A study of gamma-ray and neutron radiation in the interaction of a 2 MeV proton beam with various materials, Appl. Radiat. Isotopes 106 (2015) 38–40, https://doi.org/10.1016/j.apradiso.2015.08.011.
[9] G.M. McCracken, The behavior of surfaces under ion bombardment, Rep. Prog. Phys. 8 (1975) 241–327.
[10] R. Berish (Ed.), Sputtering by Particle Bombardment, Springer, Berlin, 1981.
[11] M.I. Guseva, Yu.V. Martynenko, Radiation blistering, Sov. Phys. Usp. 24 (1981) 996–1007.
[12] V. Astrelin, et al., Blistering of the selected materials irradiated by intense 200 keV proton beam, J. Nucl. Materials 396 (2010) 43–48, https://doi.org/10.1016/j.jnucmat.2009.10.051.
[13] K. Ono, Prospects for new era of boron neutron capture therapy and subjects for the future, Ther. Radiol. Oncol. 2 (2018) 40–46, https://doi.org/10.21037/tro.2018.09.04.
[14] T. Edgecock, J. Bennett, S. Green, B. Phoenix, M. Scott, A study of the production of neutrons for Boron Neutron Capture Therapy using a proton accelerator, Proc. IPAC2014, Dresden, Germany, WEPRO099 (2014). doi:10.18429/JACoW-IPAC2014-WEPRO099.
[15] T. Kurihara, H. Kobayashi, H. Matsumoto, M. Yoshioka, Neutron target research and development for BNCT: direct observation of proton induced blistering using light-polarization and reflectivity changes, J. Radioanal. Nucl. Chem. 305 (2015) 935–942, https://doi.org/10.1007/s10967-015-4056-y.
[16] E. Fagotti, MUNES project: status and perspectives of an RFQ based neutron facility in Italy. Symp. North Eastern Accelerator Personnel, INFN Laboratori Nazionali di

Legnaro, Italy, 2012.
[17] H. Kobayashi et al., Construction of a BNCT facility using an 8-MeV high power proton linac in Tokai, Proc. IPAC2012, New Orleans, Louisiana, USA, THPPR048, 2012.
[18] Y. Kiyanagi, Accelerator-based neutron source for boron neutron capture therapy, Ther. Radiol. Oncol. 2 (2018) 55–67, https://doi.org/10.21037/tro.2018.10.05.
[19] T.R. Armstrong, P.B. Johnson, W.R. Jones, The formation of a blistering in copper irradiated at 120 K: a stress-related phenomenon? J. Nucl. Mater. 114 (1983) 1–6.
[20] X. Liu, et al., The Kinetic Behaviors of H Impurities in the Li/Ta Bilayer: Application for the Accelerator-Based BNCT, Nanomaterials 9 (2019) 1107, https://doi.org/10.3390/nano9081107.
[21] I. Mardor et al., The Soreq Applied Research Accelerator Facility (SARAF) – Overview, Research Programs and Future Plans. ArXiv: 1801.06493, 2018. doi:10.1140/epja/i2018-12526-2.
[22] H. Koay et al., Conceptual design of compact-multichanel neutron moderator for accelerator based BNCT system, Proc. 14th Annual Meeting of Particle Accelerator Society of Japan, Sapporo, Japan, PASJ2017 WEP124, 2017.
[23] S. Ishiyama, Y. Baba, R. Fujii, M. Nakamura, Y. Imahori, Thermal stability of BNCT neutron production target synthesized by in-situ lithium deposition and ion implantation, Mater. Trans. 54 (2013) 1760–1764.
[24] T. Mitsumoto et al., Cyclotron-based neutron source for BNCT, Proc. XIV Intern. Congress on Neutron Capture Therapy, Buenos Aires, Argentina, 2010, pp. 510–522.
[25] T. Beynon, K. Forcey, S. Green, G. Cruickshank, N. James, Status of the Birmingham accelerator based BNCT facility. In: Sauerwein W., Moss R. and Wittig A. (eds.). Research and Development in Neutron Capture Therapy, Bologna: Monduzzi Editore, Intern. Proc. Division (2002) 225–228.
[26] O.E. Kononov, V.N. Kononov, A.N. Solovev, M.V. Bokhovko, Accelerator-based source of epithermal neutrons for neutron capture therapy, Atomic Energy 97 (2004) 626–631, https://doi.org/10.1007/s10512-005-0043-7.
[27] C. Willis, J. Lenz, D. Swenson, High-power lithium target for accelerator-based BNCT. Proc. XXIV Linear Accelerator Conference, Victoria, British Columbia, Canada (2008) 223-225.
[28] M. Yoshioka, Review of accelerator-based boron neutron capture therapy machines. Proc. IPAC2016, Busan, Korea, THXB01 (2016).
[29] A. Badrutdinov, et al., In situ observations of blistering of a metal irradiated with 2-MeV protons, Metals 7 (2017) 558, https://doi.org/10.3390/met7120558.
[30] B. Bayanov, E. Zhurov, S. Taskaev, Measuring the lithium thickness, Instrum. Exp. Techn. 51 (2008) 147–149, https://doi.org/10.1134/S002044120801020X.
[31] C.L. Lee, X.-L. Zhou, Thick target neutron yields for the ^{7}Li(p, n)7Be reaction near threshold, Nucl. Instrum. Meth. B 152 (1999) 1–11.
[32] H. Andersen, J. Ziegler, Hydrogen stopping powers and ranges in all elements. Volume 3 of the stopping and ranges of ions in matter, Pergamon Press Inc., 1977.
[33] L. Zaidi, M. Belgaid, S. Taskaev, R. Khelifi, Beam shaping assembly design of ^{7}Li(p, n)7Be neutron source for boron neutron capture therapy of deep-seated tumor, Appl. Radiat. Isotopes 139 (2018) 316–324, https://doi.org/10.1016/j.apradiso.2018.05.029.
[34] A.V. Panchenko, N.D. Tolstykh, S.A. Gromilov, The technique of X-ray diffraction investigation of crystal aggregates, J. Structural Chemistry 55 (2014) 1209–1214, https://doi.org/10.1134/S002247661407004X.
[35] W. Klemm, B. Volavszek, Zur kenntnis des systems lithium–kupfer, Z. Anorg. Allg. Chem. 296 (1958) 184–187.
[36] A.V. Brown, Development of High-power Producing Lithium Target for Boron Neutron Capture Therapy, Ph.D. Thesis University of Birmingham, UK, 2000.